



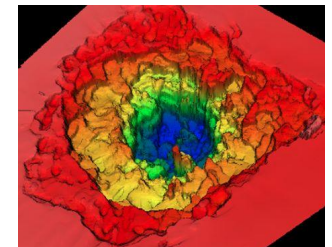
NANOPLASMONICS FOR LASER ASSISTED NUCLEAR FUSION

NORBERT KROO
(on behalf of the NAPLIFE project, Budapest)
WIGNER RESEARCH CENTER OF PHYSICS



HUNGARIAN NATIONAL
LABORATORY

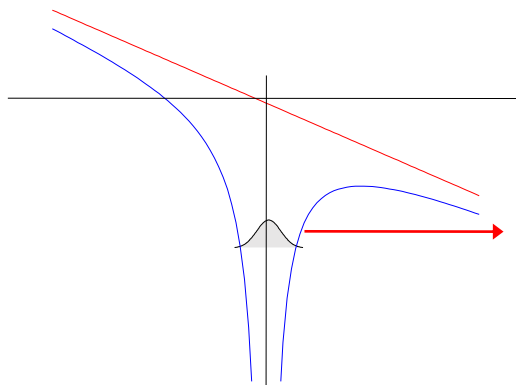
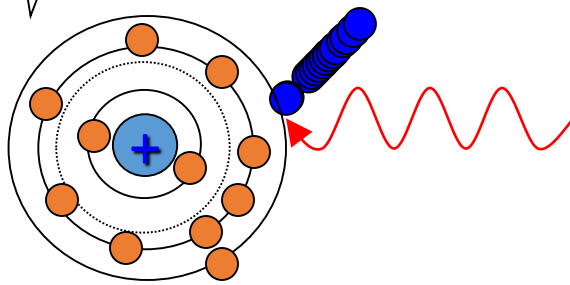
OAK: 03.09.2024



1. Materials under extreme conditions

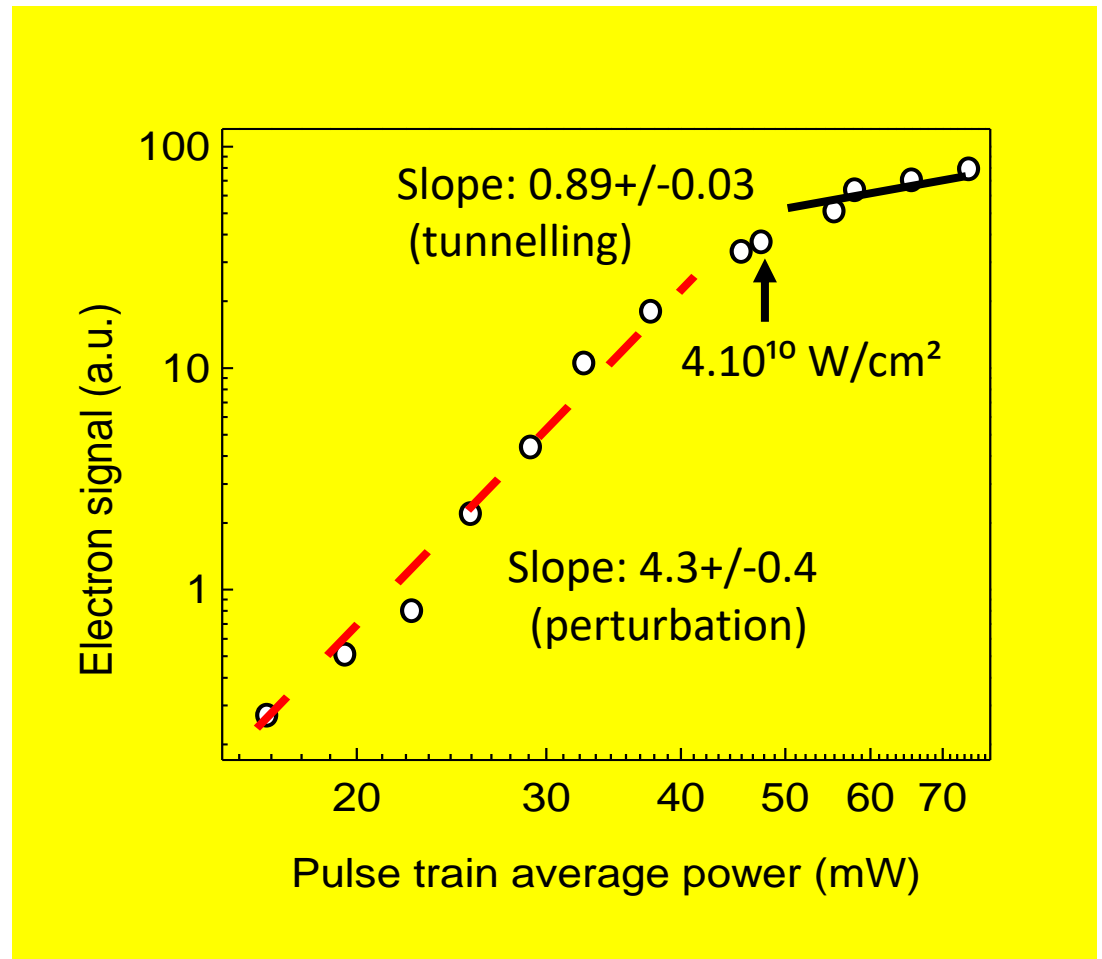


$I = 10^{16} \text{ W cm}^{-2}$



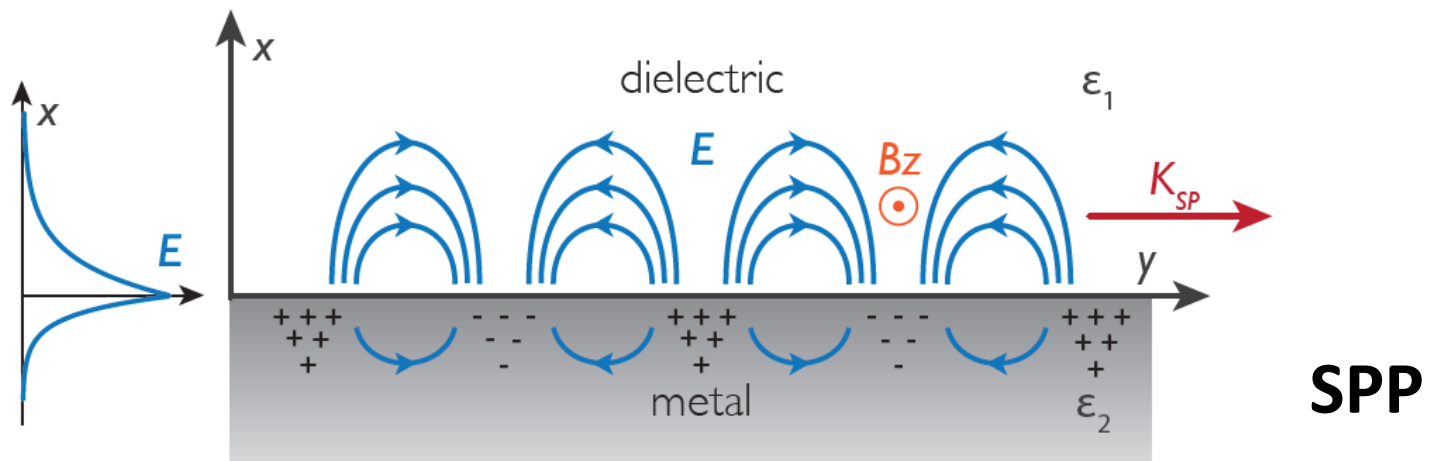
Tunnelling

$10^{14} - 10^{15} \text{ W cm}^{-2}$

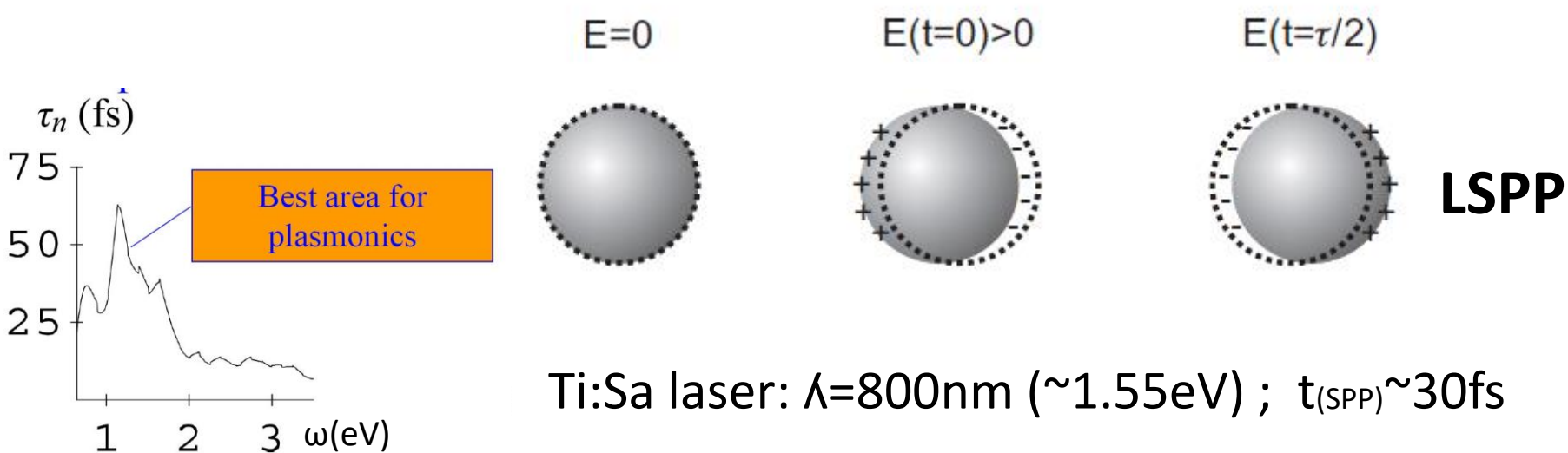


2.PLASMONICS AND HIGH FIELDS APPLICATIONS

Special type of the optical near field



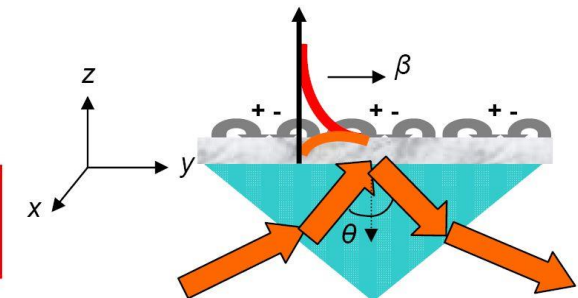
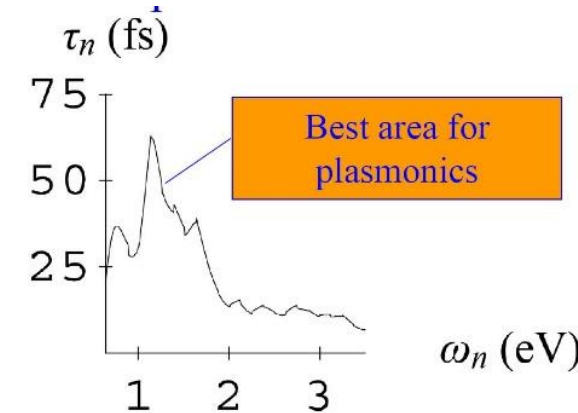
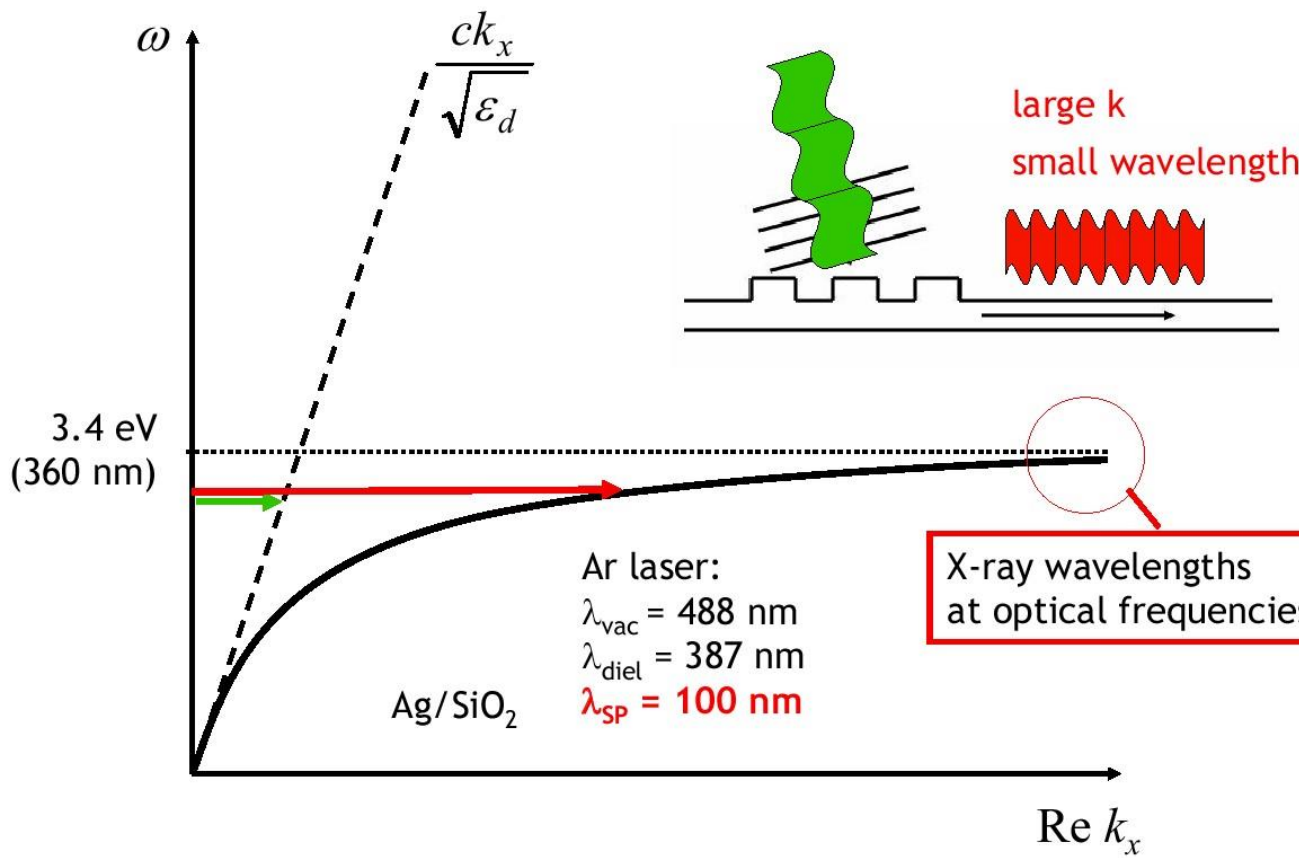
SPP



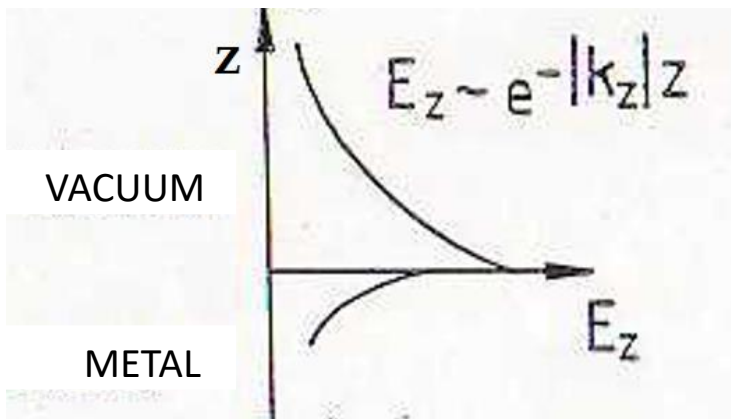
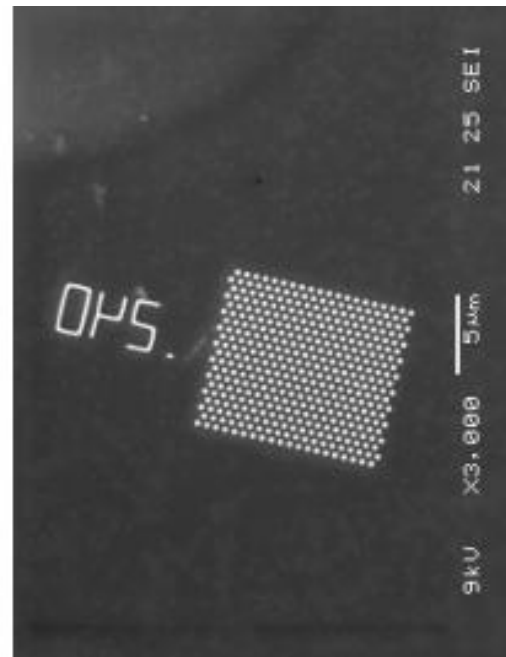
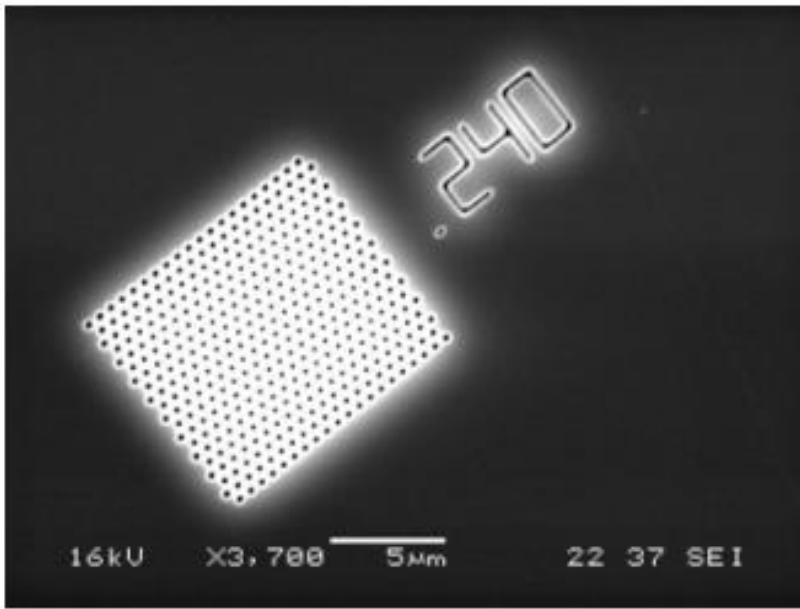


SURFACE PLASMON POLARITONS (SPP)

Surface plasmons dispersion: $k_x = \frac{\omega}{c} \left(\frac{\epsilon_m \epsilon_d}{\epsilon_m + \epsilon_d} \right)^{1/2}$



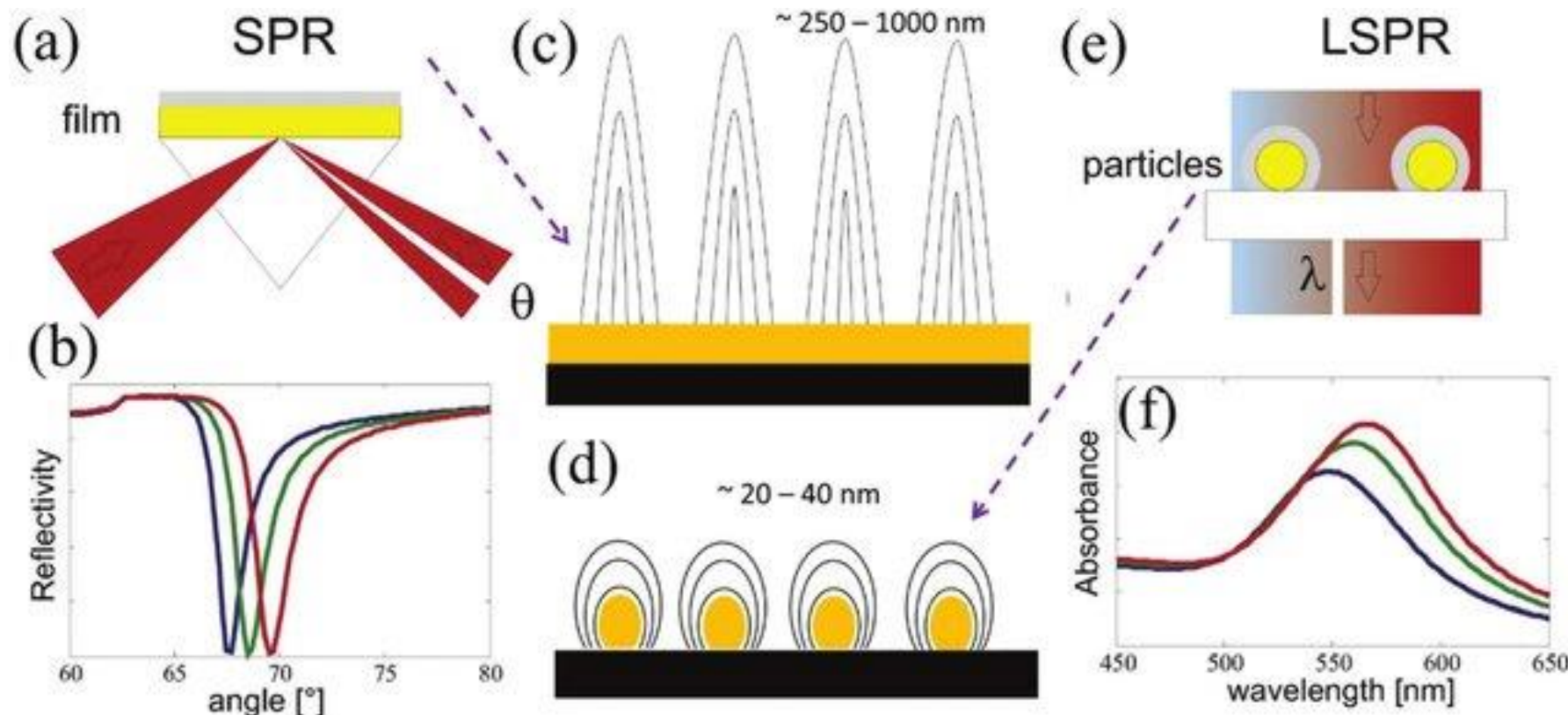
Light gets through holes, much smaller than the wavelength.



**MOST OF THE ENERGY IS CONCENTRATED AT THE SURFACE:
GIANT FIELD AMPLIFICATION
MANY POTENTIAL APPLICATIONS.**

2.LOCALIZED PLASMONS (LSPP) UP TO 10^{20} W/cm²)

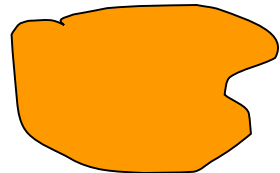
(The basic difference between SPP-s and LSPP-s)



- NO PENETRATION INTO THE PLASMONIC MATERIAL (e.g. metal)
- SMALLER PENETRATION INTO THE DIELECTRIC /VACUUM
- NO DISPERSION, RESONANCE DEPENDS ON SIZE, SHAPE, MATERIAL
- BROADER RESONANCE

PLASMON RESONANCE OF NANOPARTICLES SHAPE AND- ÉS SIZE DEPENDENT!

$$\omega_B = \sqrt{\frac{4\pi e^2 n}{m_e}}$$



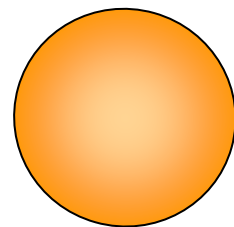
Bulk

$$\omega_{surf} = \frac{\omega_B}{\sqrt{2}}$$



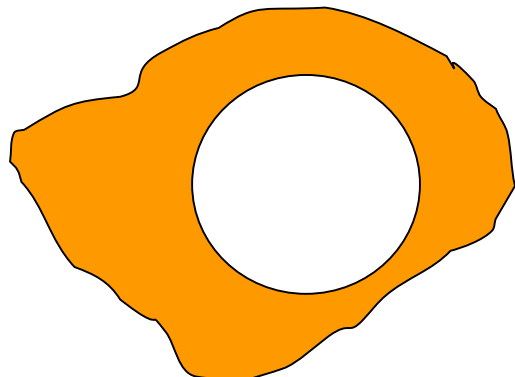
Surface

$$\omega_{S,l} = \omega_B \sqrt{\frac{l}{2l+1}}$$



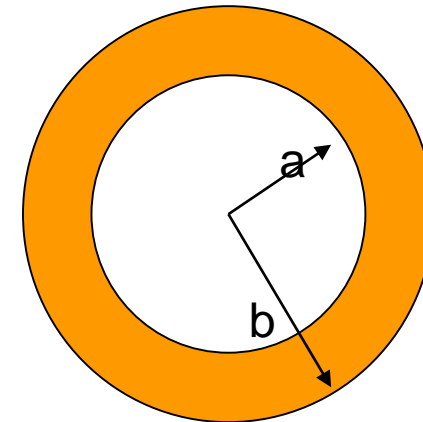
Sphere

Üreg



$$\omega_{C,l} = \omega_B \sqrt{\frac{l+1}{2l+1}}$$

Nanoshell:



$$x = \frac{a}{b}$$

$$\omega_{l\pm}^2 = \frac{\omega_B^2}{2} \left[1 \pm \frac{1}{2l+1} \sqrt{1 + 4l(l+1)x^{2l+1}} \right]$$

Nanoshell plasmon resonance depends on the x ratio .

- HOT SPOT
- SCREENING
- PONDEROMOTORIC ACCELERATION
- CORRELATED MOTION

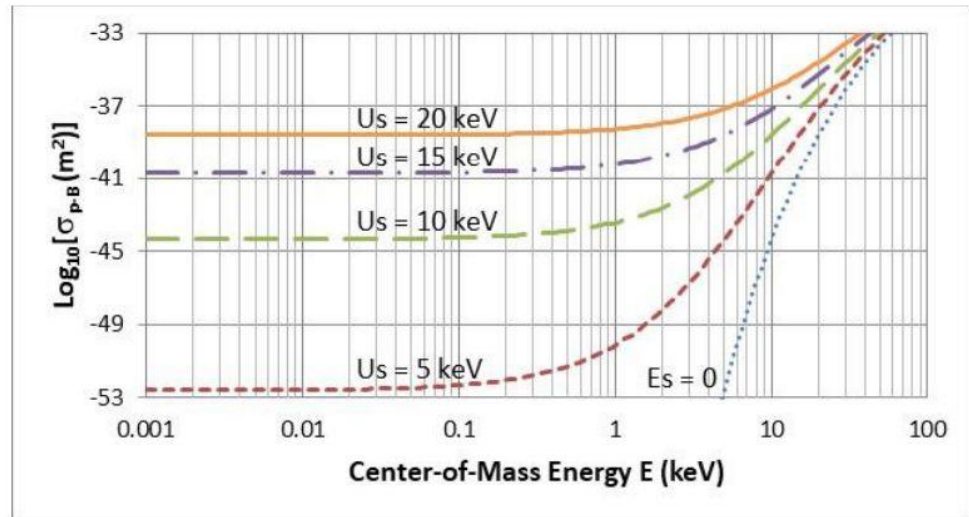
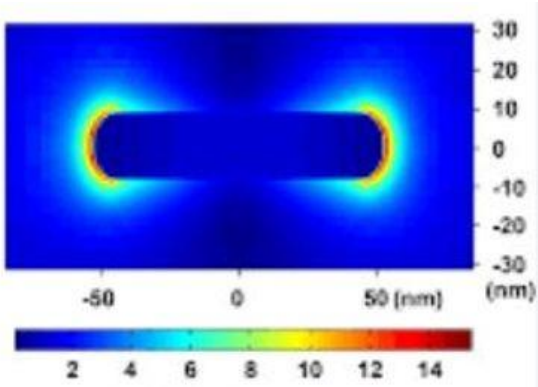
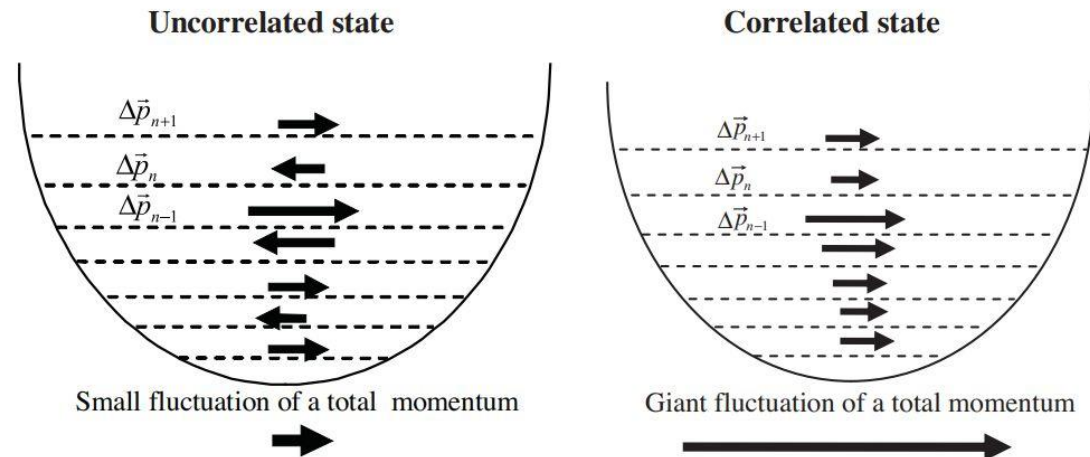
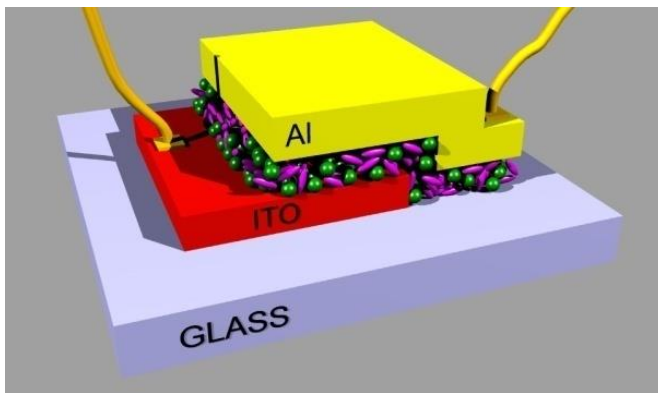


Figure 1: $p-^{11}B$ cross section as function of particle energy for the screening electron densities up to $E_s = 20\text{keV}$. The cross section near $E = 10\text{eV}$ grows over 14 orders of magnitude (from 10^{-53} to 10^{-39}m^2) over the range of 5 to 20keV.

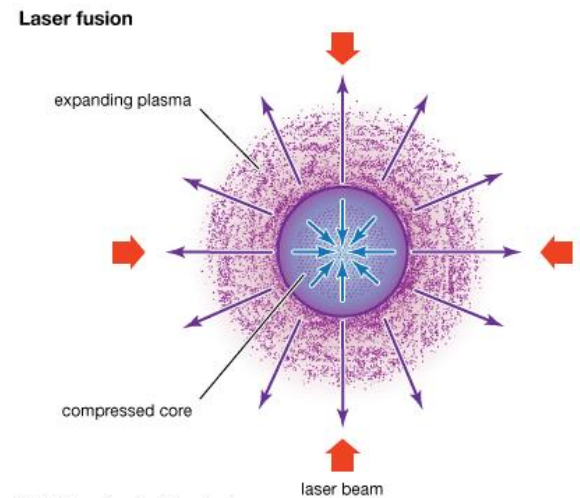
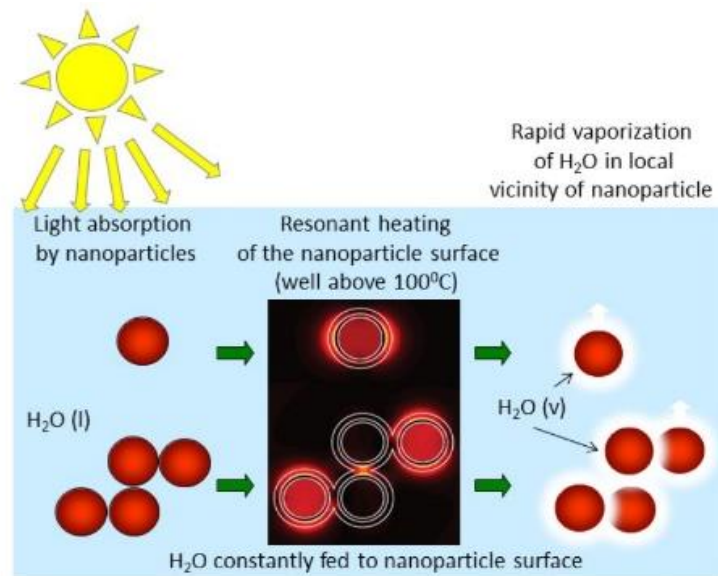
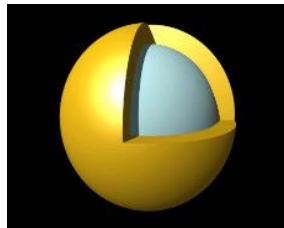
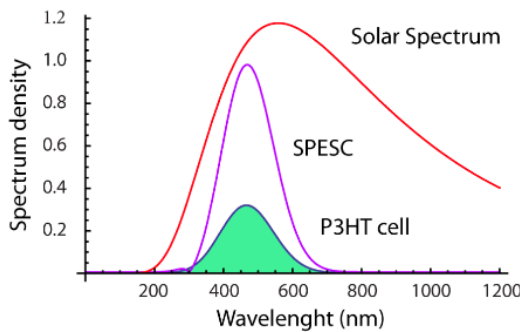


Some potential new energy technologies

(involving nanotechnologies)



P3HT Cell
efficiency = 6%
SPESC (P3HT)
efficiency = 17.5%

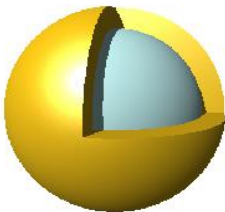


NIF (LASER INDUCED FUSION)



192 laser, 400MJ, on target 2MJ. The generated nuclear energy 3MJ. The cost of one capsule $\sim 10^5$ USD. The length of the laser pulse : 10-50ns , 1 imp/day. Facility cost: multibillion USD.

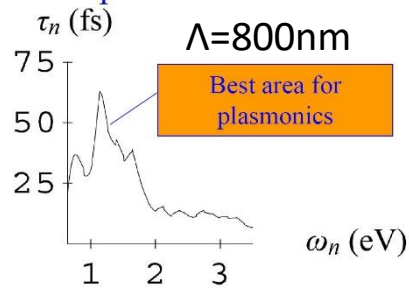
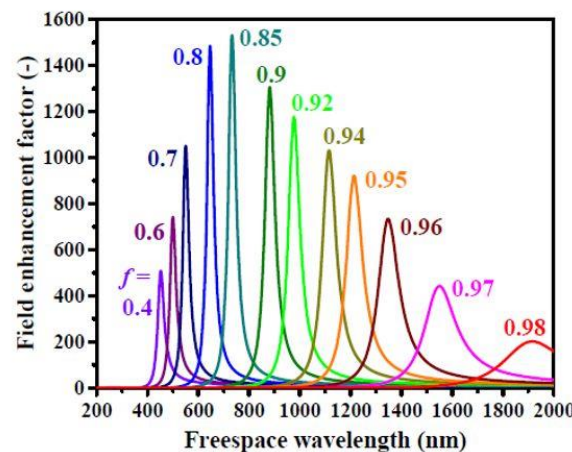
NANOPLASMONICS AND ENERGY CONCENTRATION



NANOSHELL
(nx10nm)

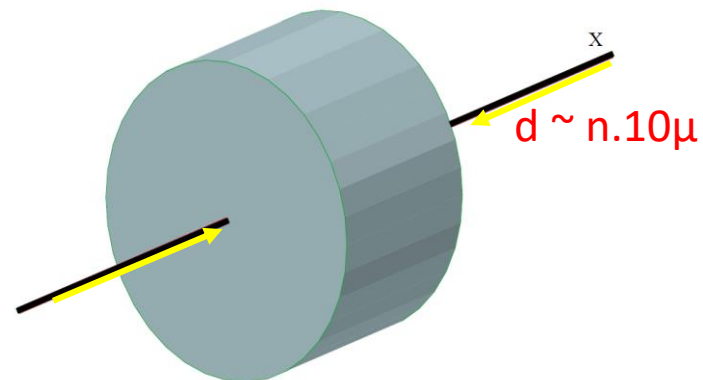


NANOROD ($\sim 85 \times 25 \text{ nm}$)



$n.10\mu$

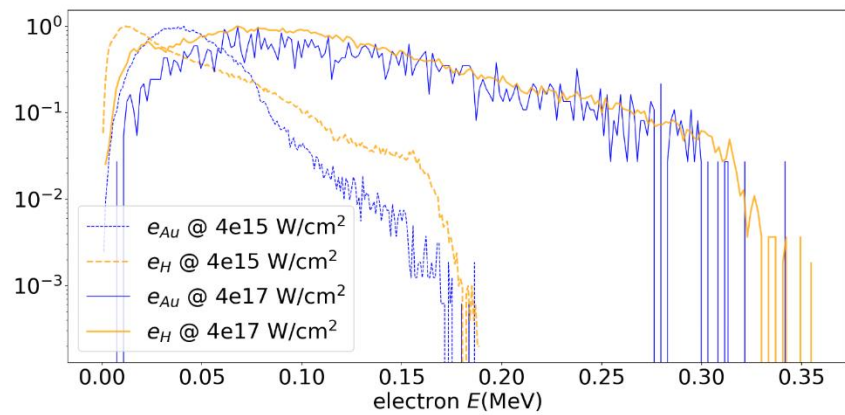
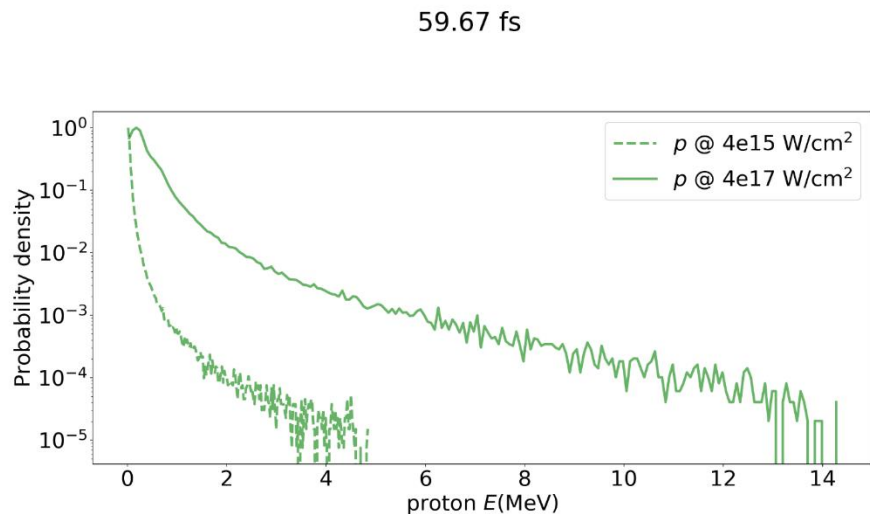
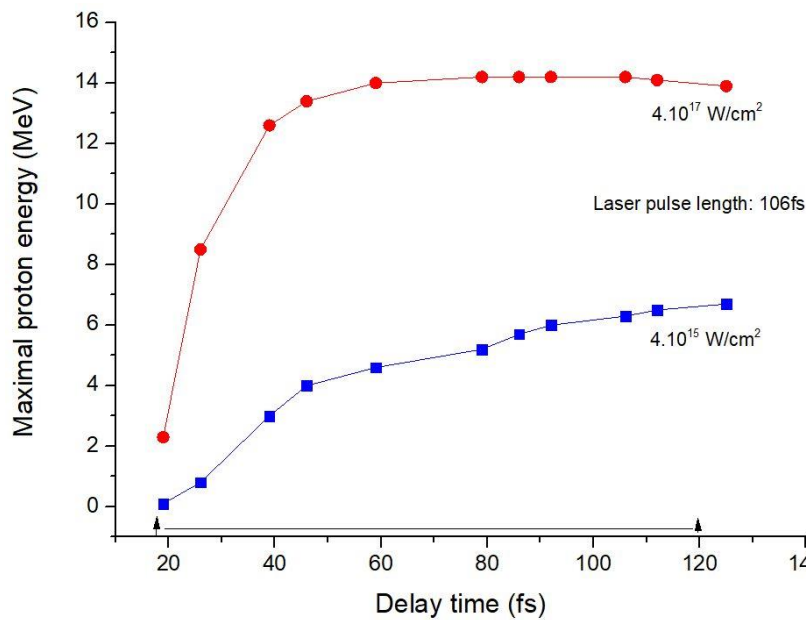
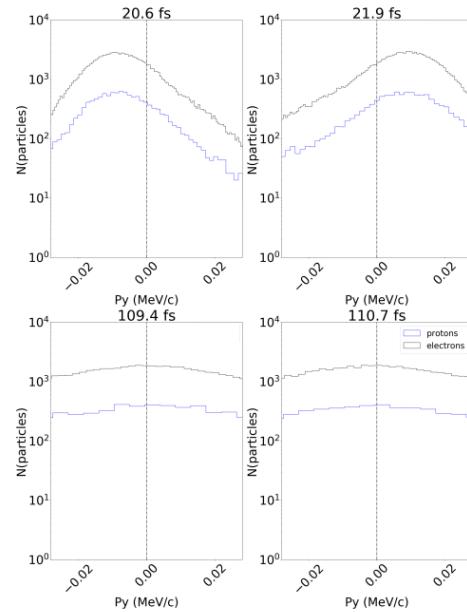
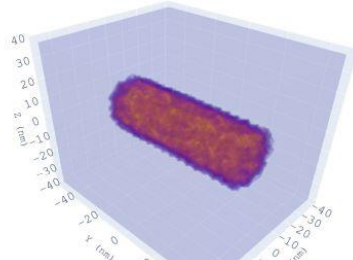
NANOPARTICLES IN
THE FUSION MATERIAL



FEMTOSECOND LASER PULSES;
HIGH REPETITION FREQUENCY;
LIGHT SPEED: NO TIME FOR
INSTABILITIES; ONLY TWO BEAMS;
TIMELIKE VOLUME IGNITION

SIMULATION OF PROTON AND ELECTRON ENERGIES AT A SINGLE NANOROD

Nanorod inside a PIC simulation box



AND UP TO $\sim 10^{20}$ W/cm²

a)

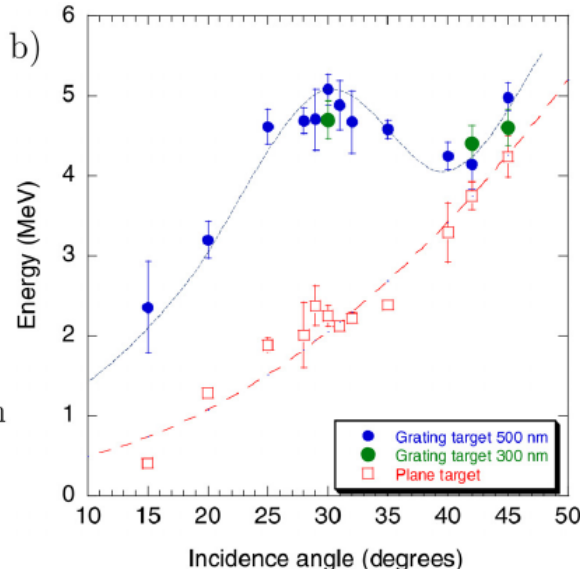
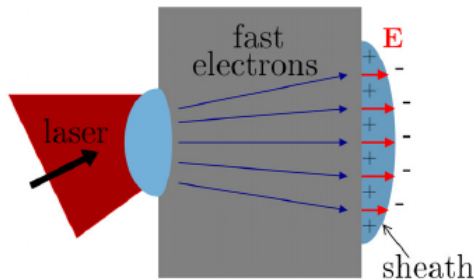


FIG. 5. Plasmon-enhanced TNSA of protons.⁹⁵ (a) Schematic of TNSA. The fast electrons produced by the interaction at the front side cross the target and produce a sheath at the rear side, where ions are accelerated. (b) Experimental data from the interactions of a high contrast 25 fs, 2.5×10^{19} W cm⁻² laser pulse with solid plastic targets. The cut-off energy of protons emitted from the rear measured as a function of the incidence angle from both flat and grating targets (for two different values of the grating depth). An up to 2.5-fold energy increase is observed for gratings, with a broad maximum around the resonant angle for SP excitation (30°). Data from Ref. 95.

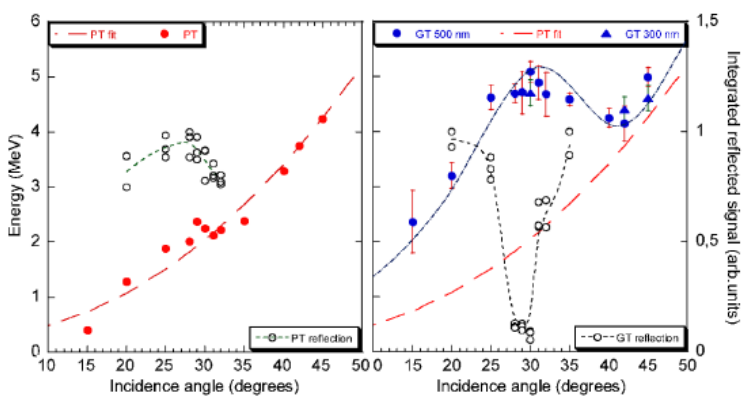


FIG. 3 (color online). Maximum proton energy (filled data points) and reflected light signal (empty data points) as a function of incidence angle α . Left and right frames correspond to 20 μm thick plane targets and to 23 μm thick grating targets, respectively. Filled circles and triangles correspond to 0.5 and 0.3 μm deep gratings, respectively. The (red) dashed line is proportional to $\sin^2 \alpha / \cos \alpha$. The other lines are guides for the eye.

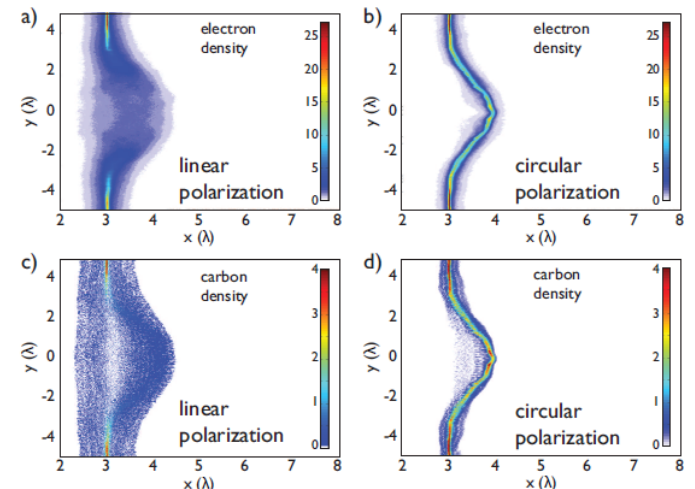
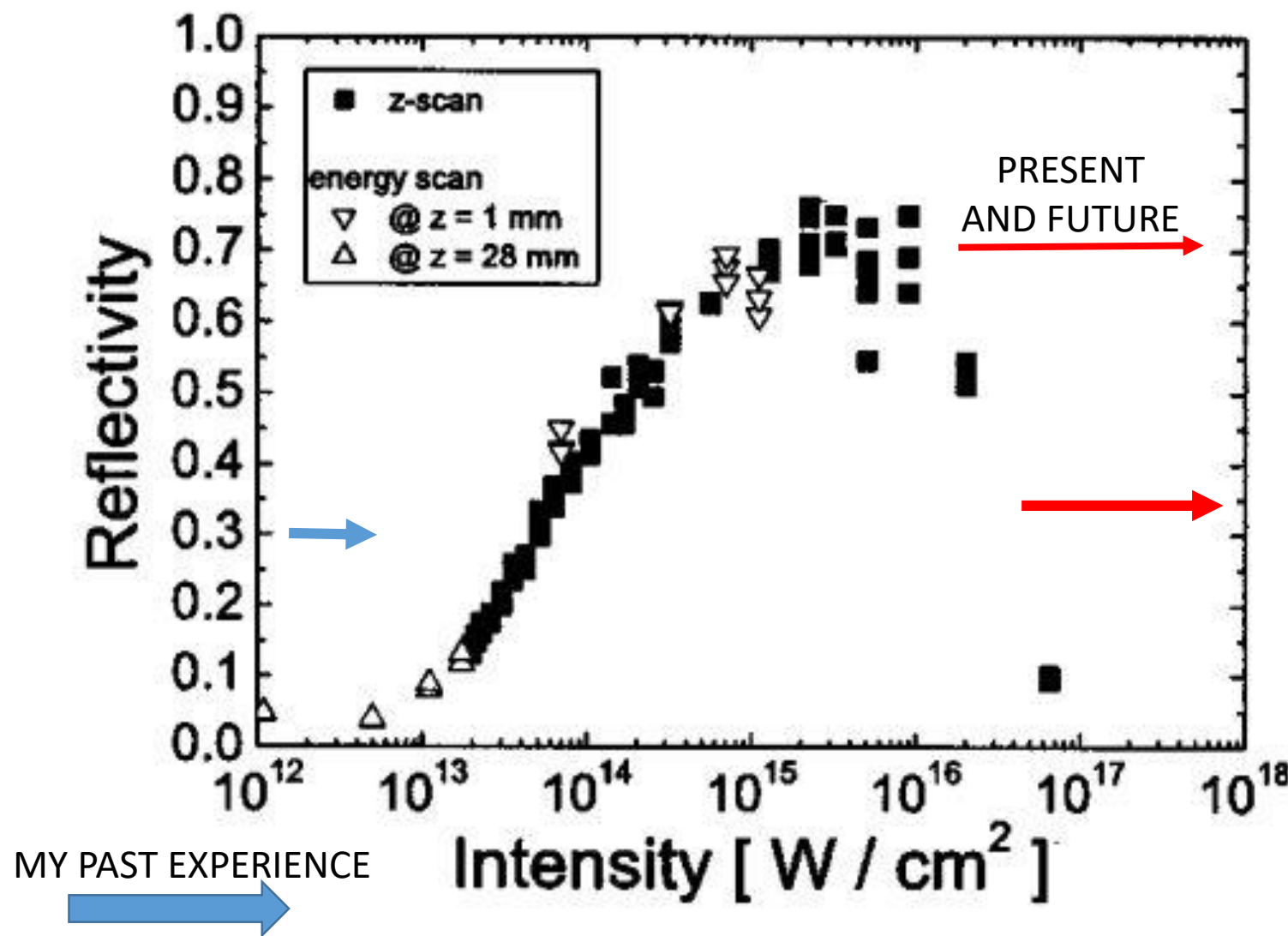
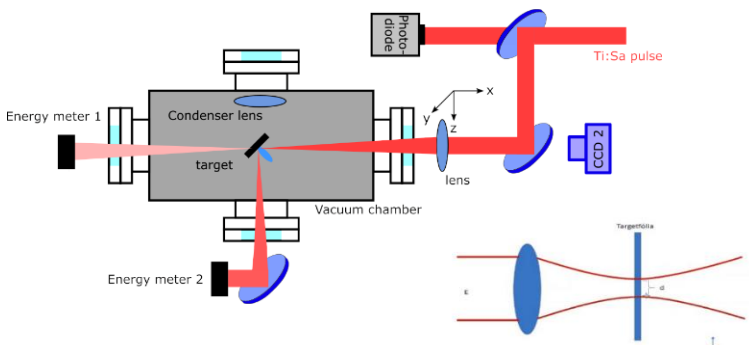
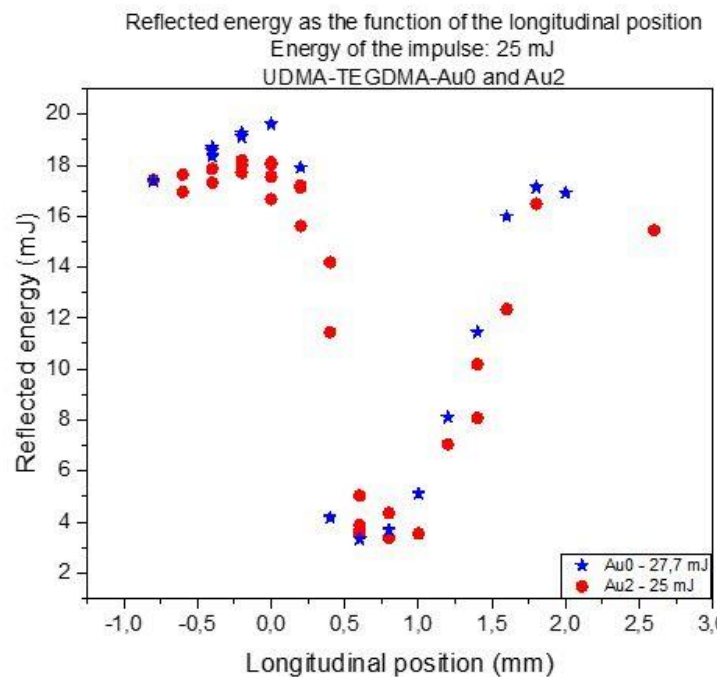
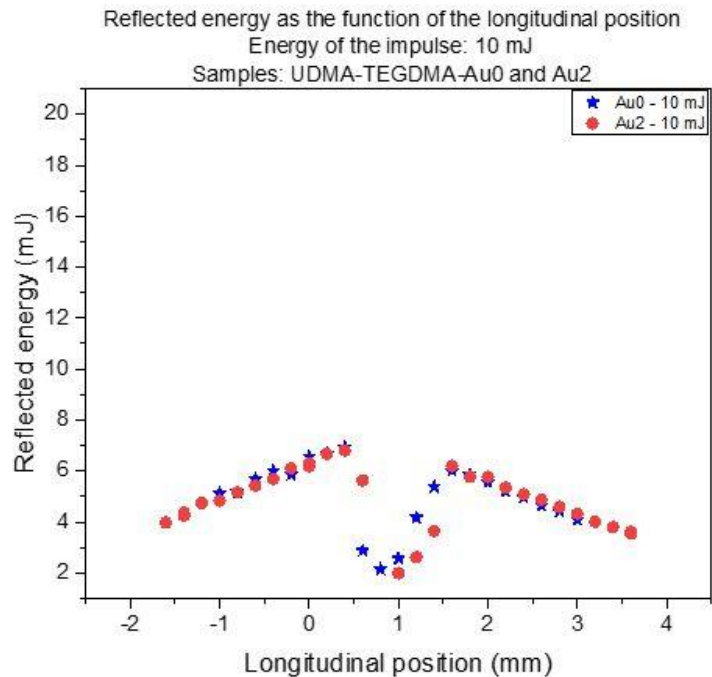


FIG. 4: (color). Cycle-averaged electron (a,b) and carbon ion (c,d) density at $t = 61$ fs after the peak of the laser pulse reached the 5.3 nm target initially located at $x = 3\lambda$. While linear polarization results in strong expansion of the target caused by hot electrons, for circularly polarized irradiation the foil is accelerated as a dense, quasi-neutral plasma bunch.

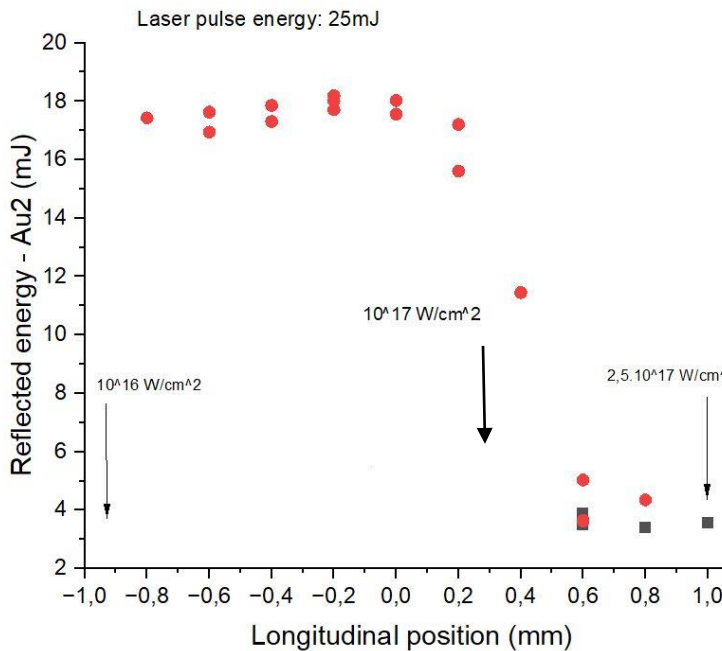
LIGHT-MATTER INTERACTION:
PLASMA-MIRROR REFLECTIVITY
(how can light enter into matter?)

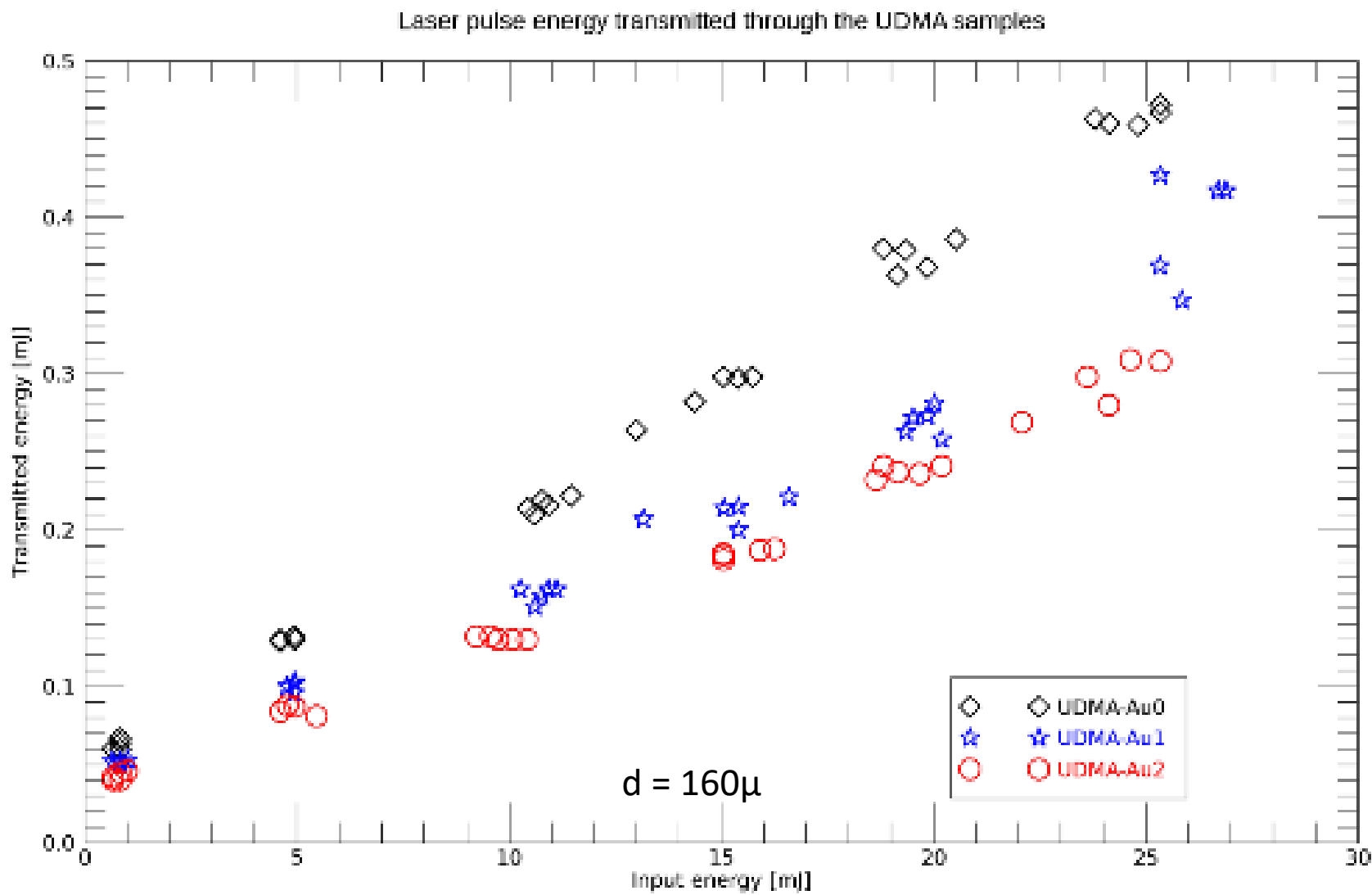




MEASUREMENTS AT WIGNER R.C.

Sample: polymer (UDMA+ TEGDMA) Au2 (0.18m/m%) resonant nanorods and Au0 (without nanorods)

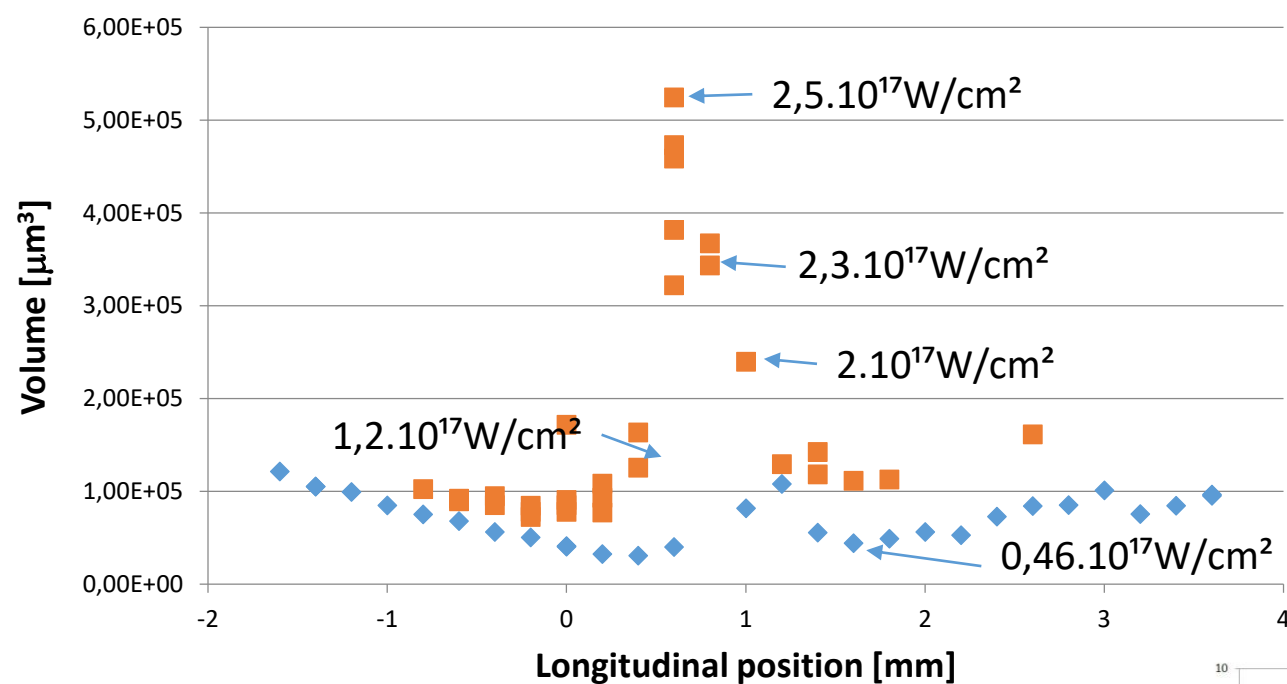




Laser pulse: 25mJ, 40fs

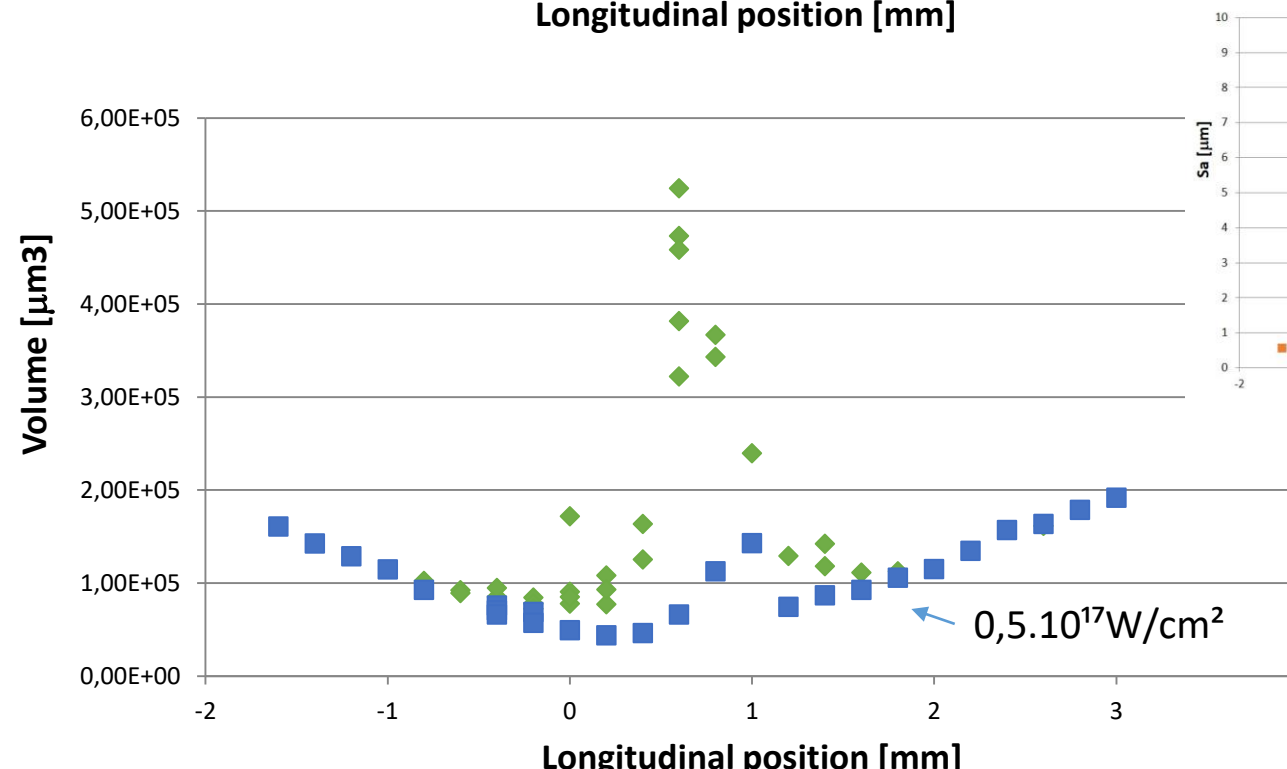
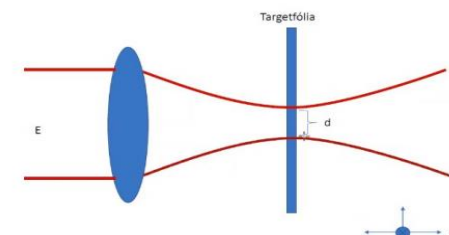
Au0	0.00 m/m%
Au1	0.12 m/m%
Au2	0.18 m/m%

CRATER VOLUMES



Volume Au2 - 10 mJ

Volume Au2 - 25 mJ

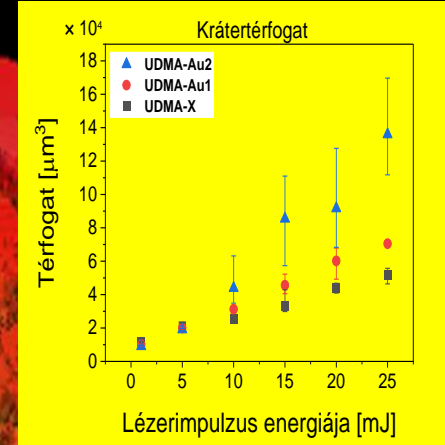


Volume - Au2 - 25 mJ
Volume - Au0 - 27,7 mJ

HIGH FIELD
PLASMONICS WORKS!

$1,2 \cdot 10^{17} \text{ W/cm}^2$

Volume $\sim 3,5 V_0$

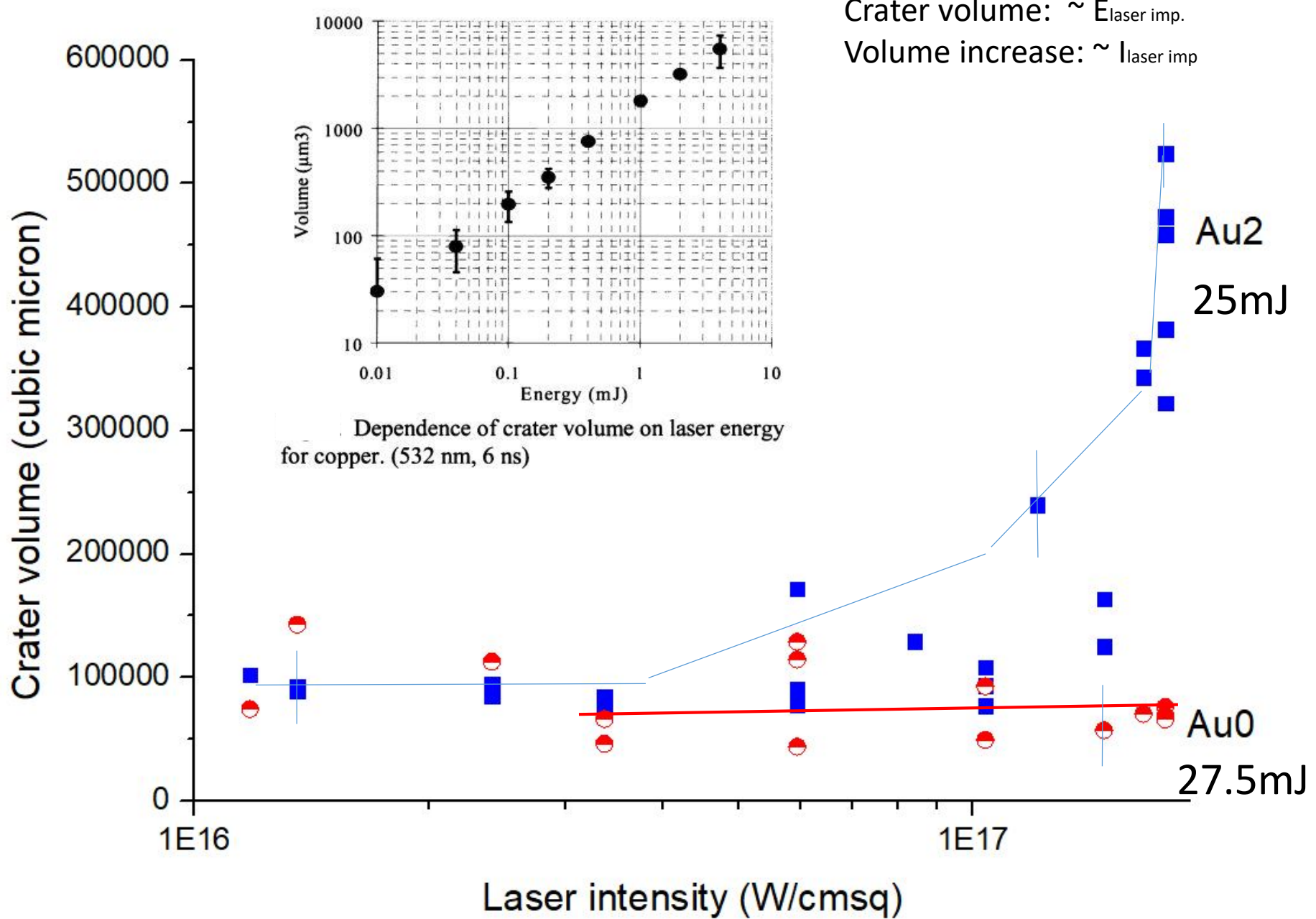


Volume: V_0

40 unit

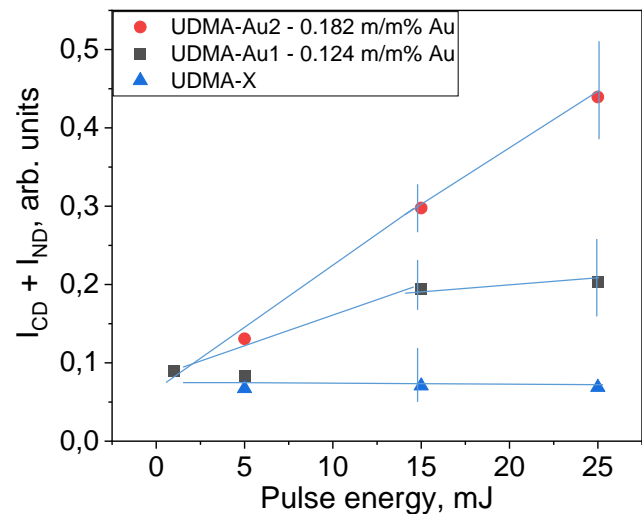
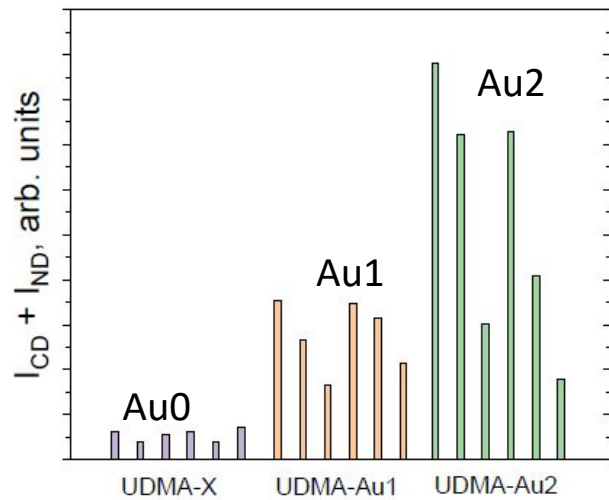
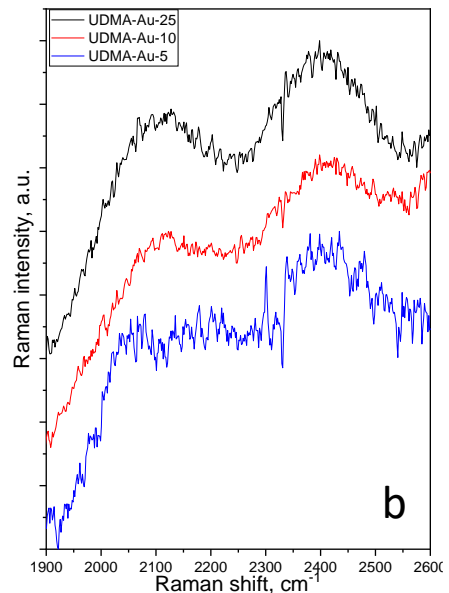
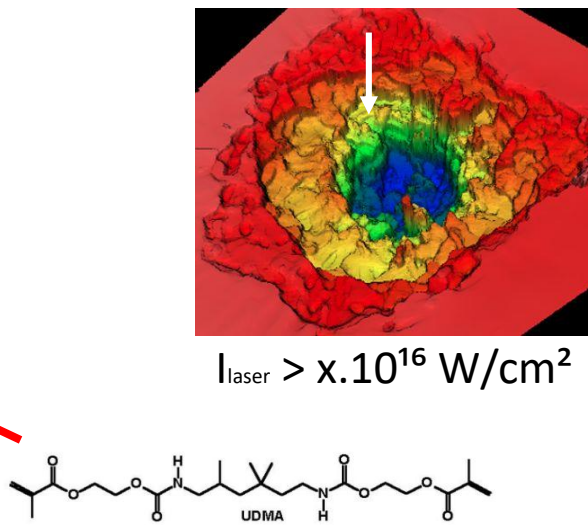
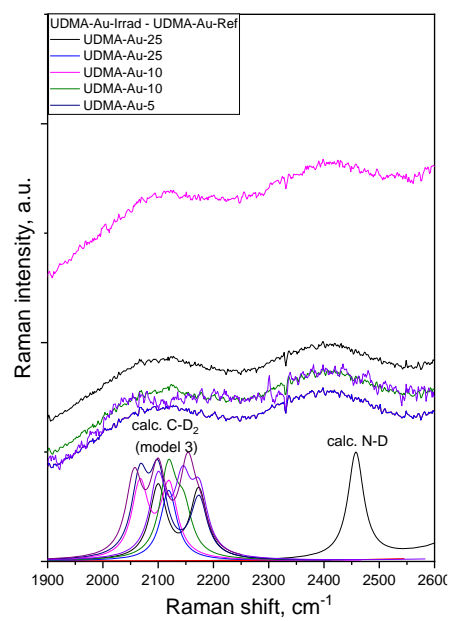
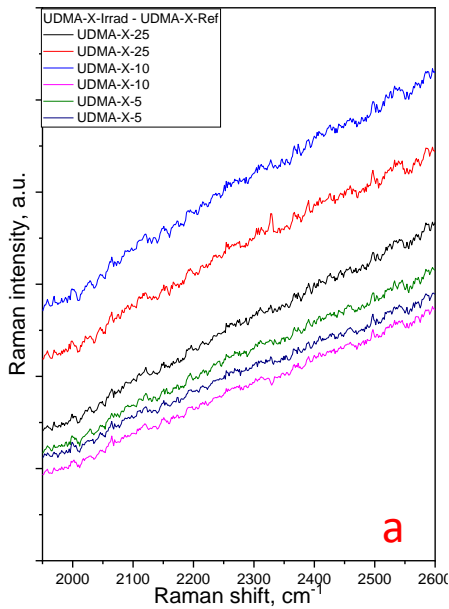


40 unit

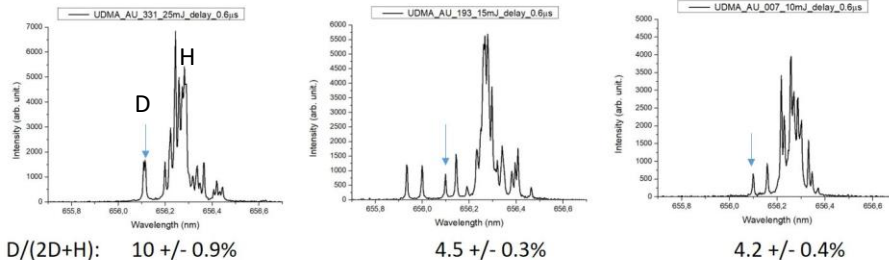


2. Diagnozis : Raman scattering from the crater surface

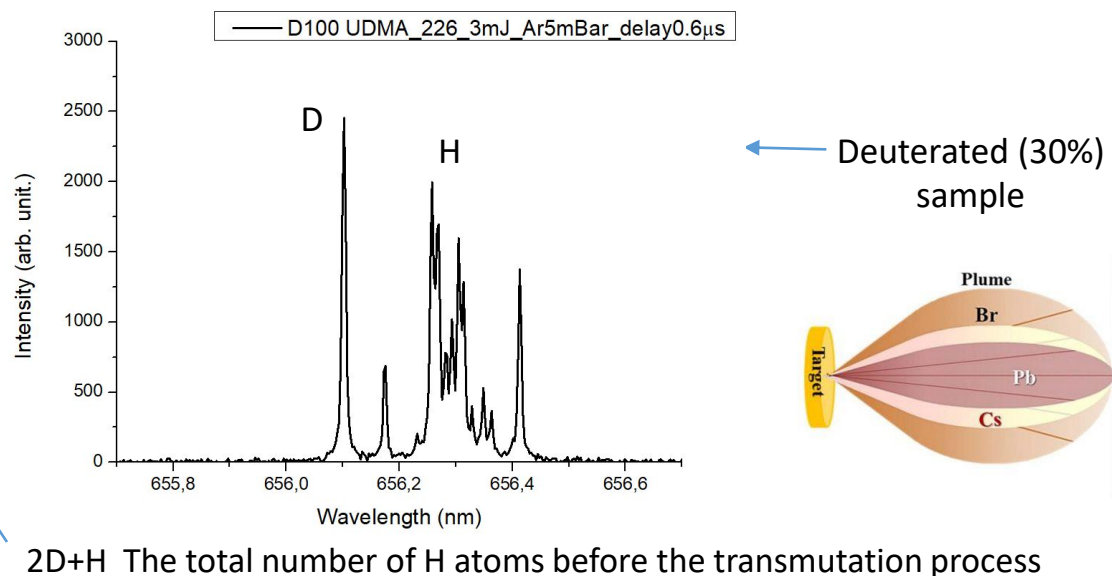
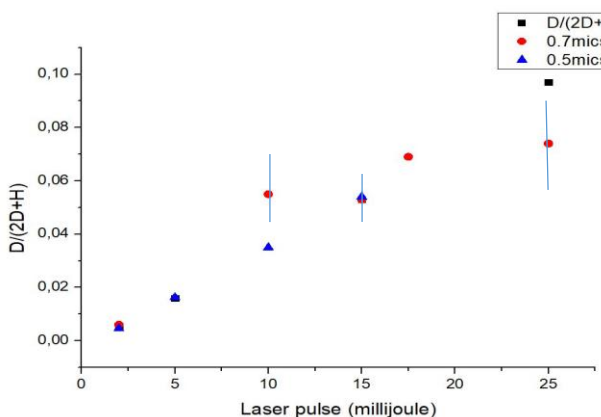
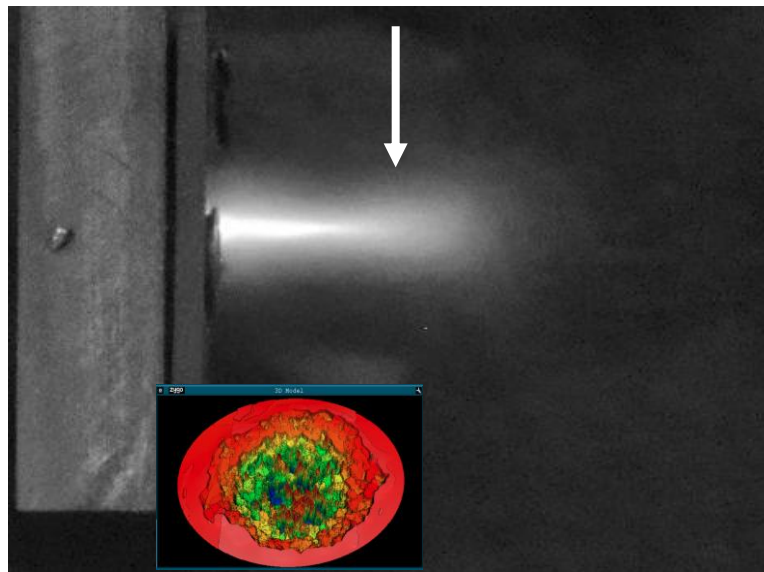
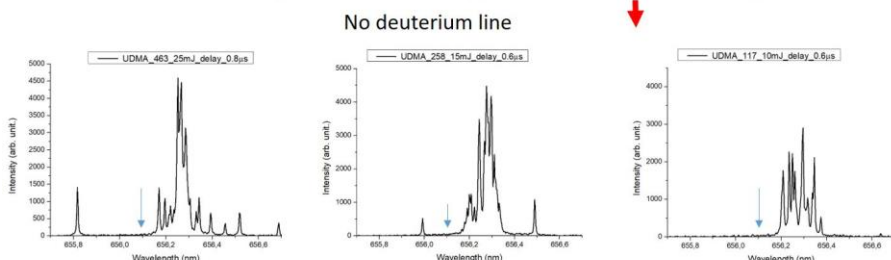
arXiv2210.00619(2022), submitted



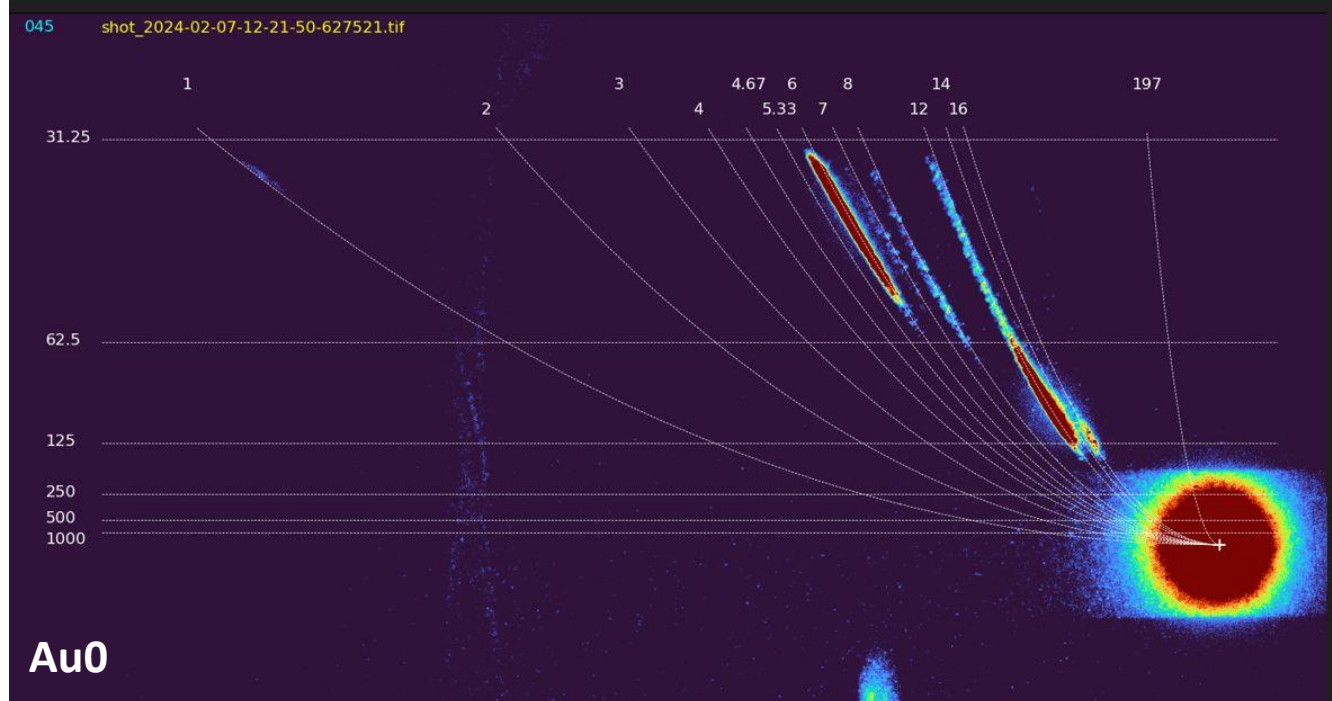
3.SOME RESULTS OF THE H^a AND D^a SPECTRAL LINES



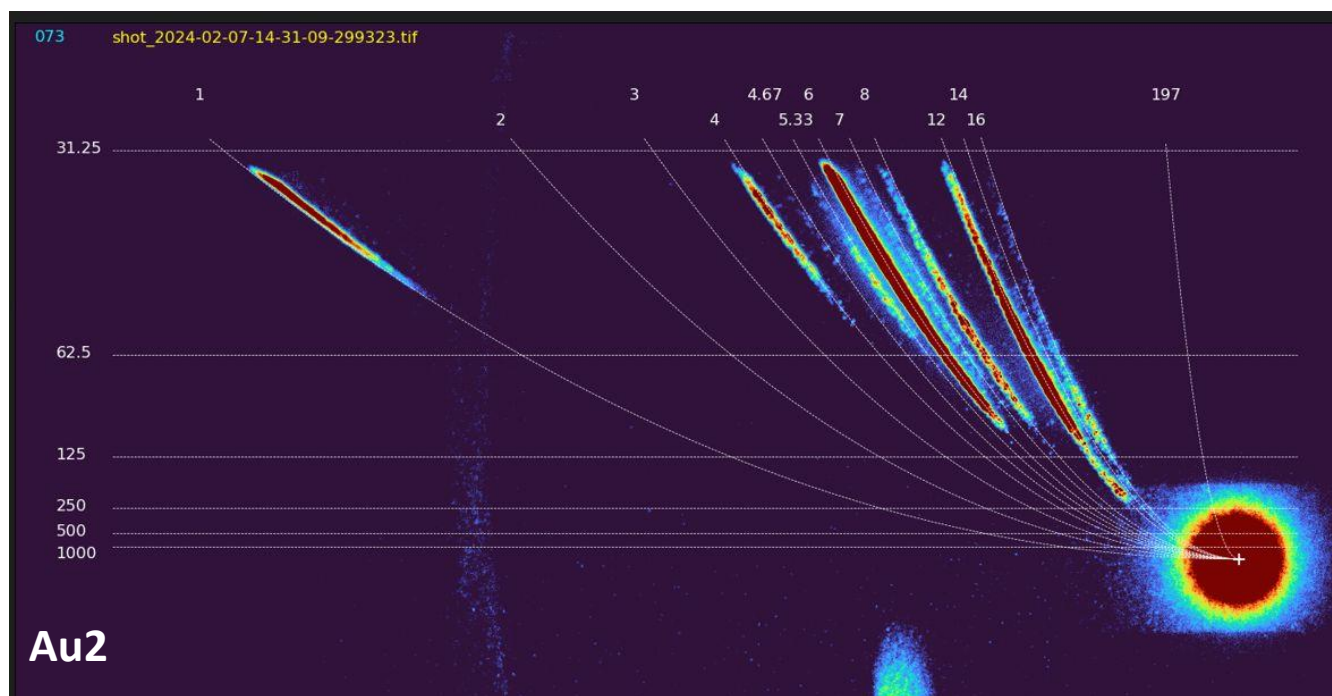
TYPICAL LIBS SPECTRA (at 3 laser pulse energies with and without Au nanoparticles)



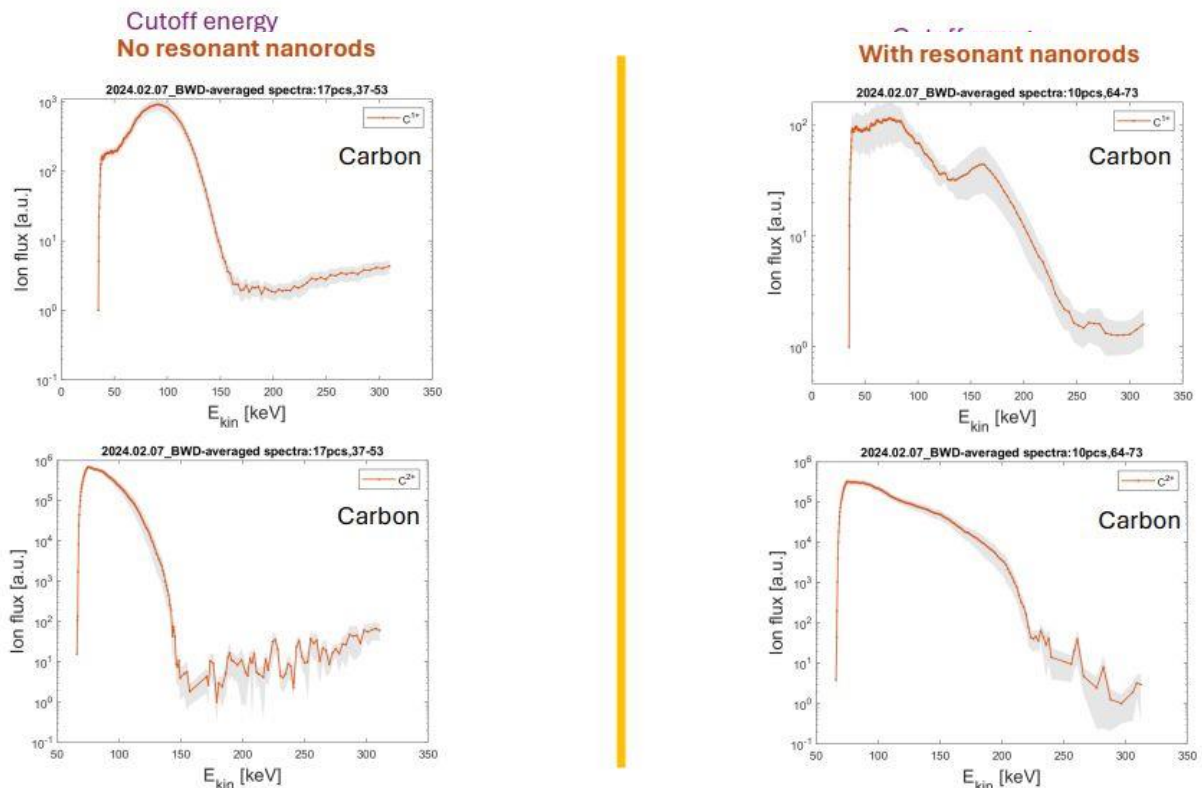
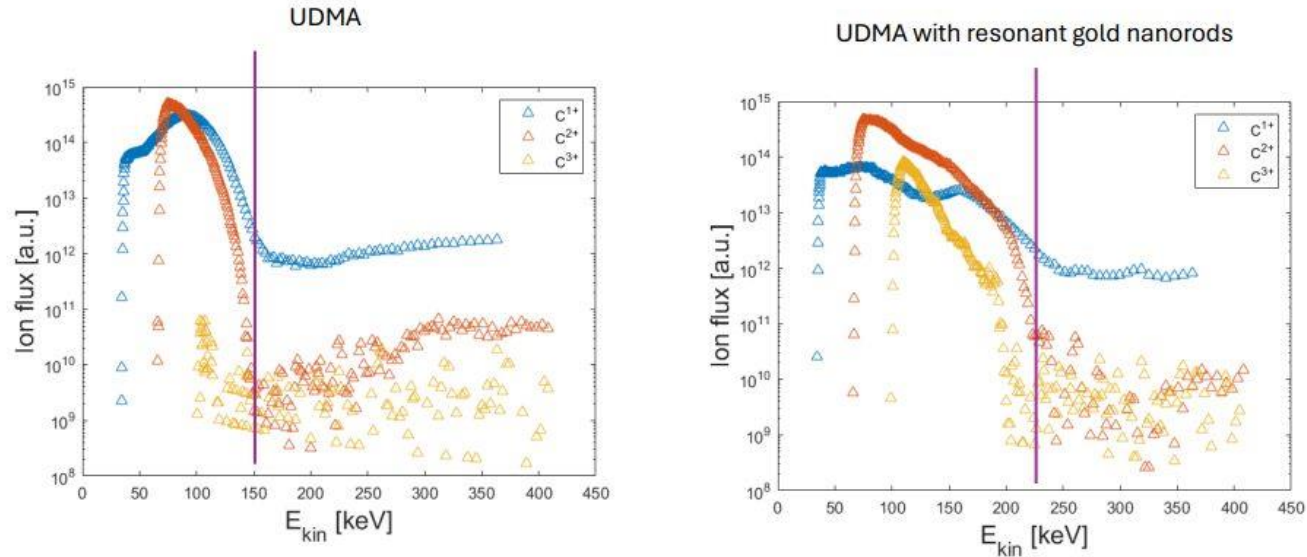
ELI-ALPS
Szeged



Thompson
parabola
measurements

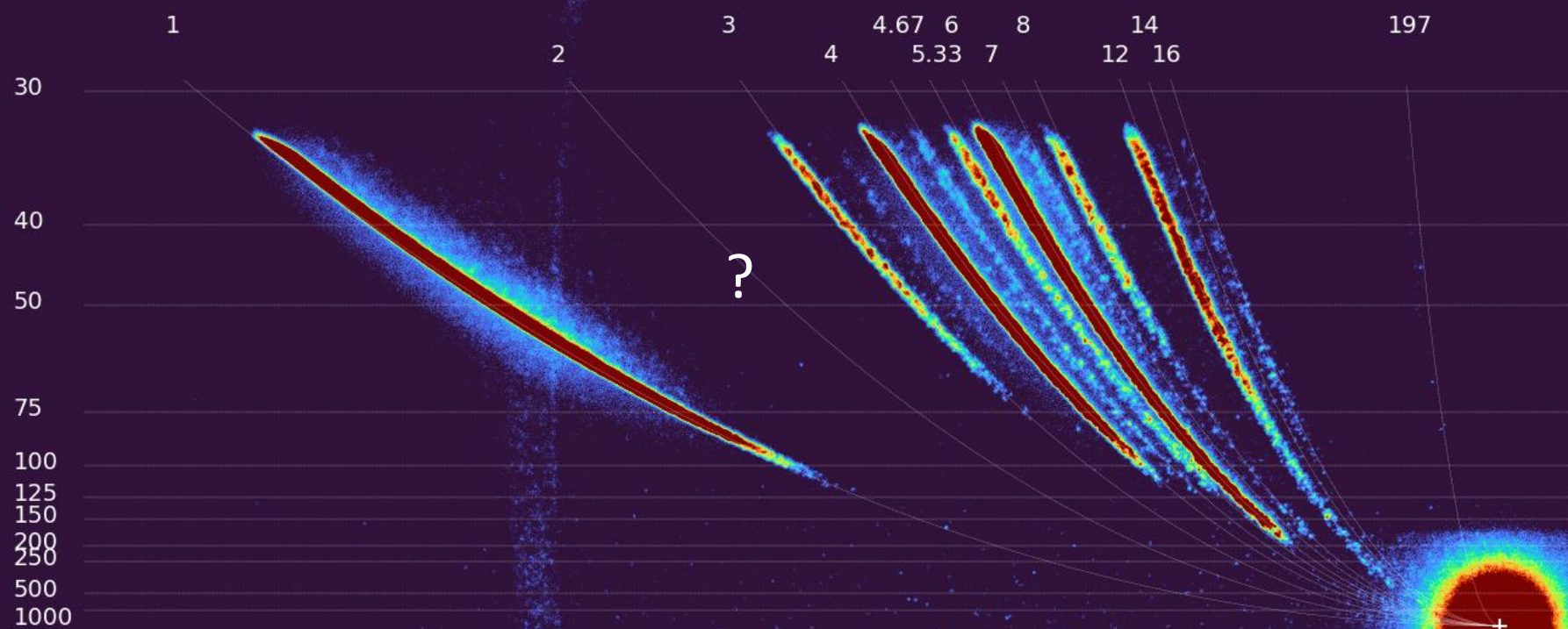


HIGH INTENSITY PLASMONICS WORKS

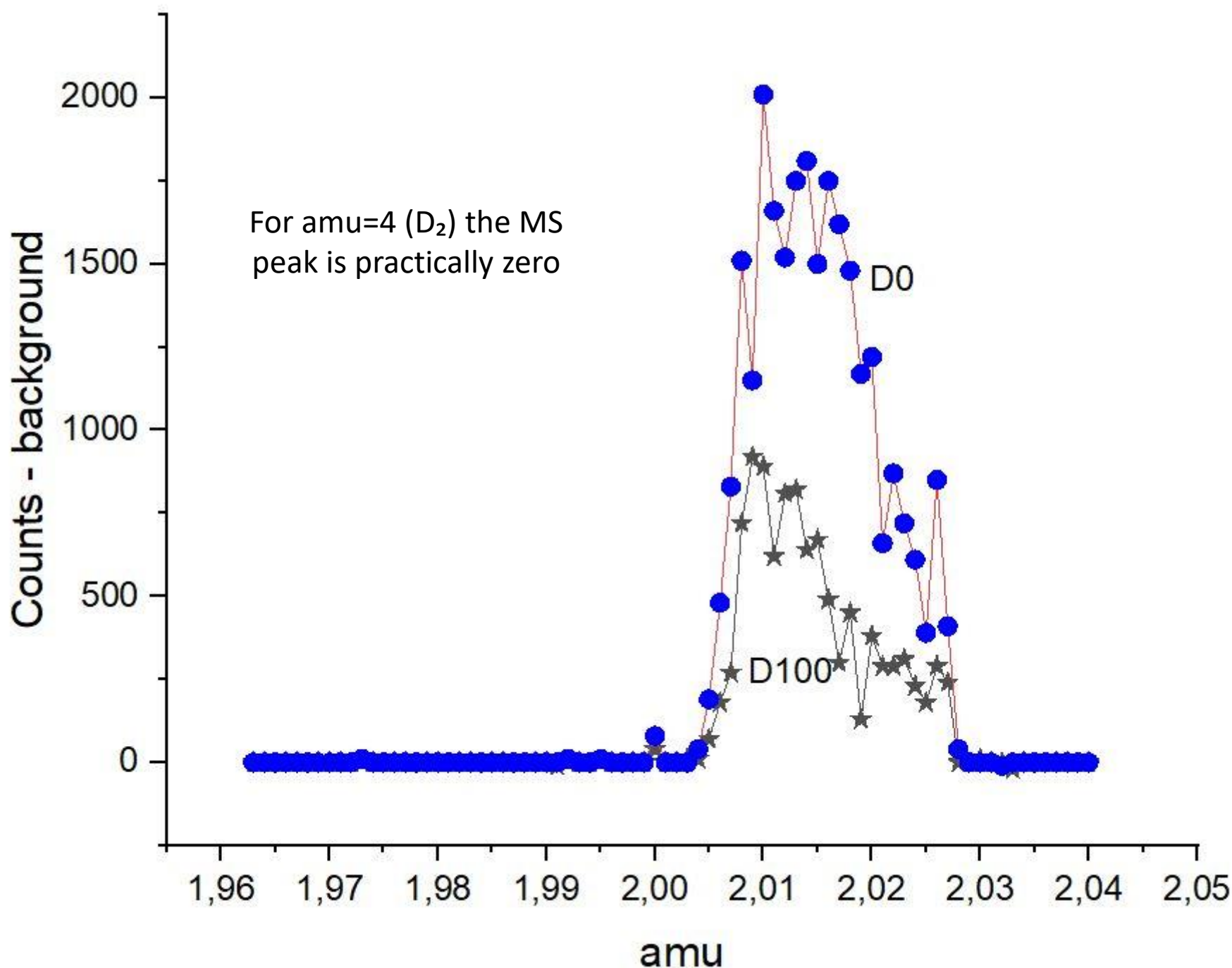


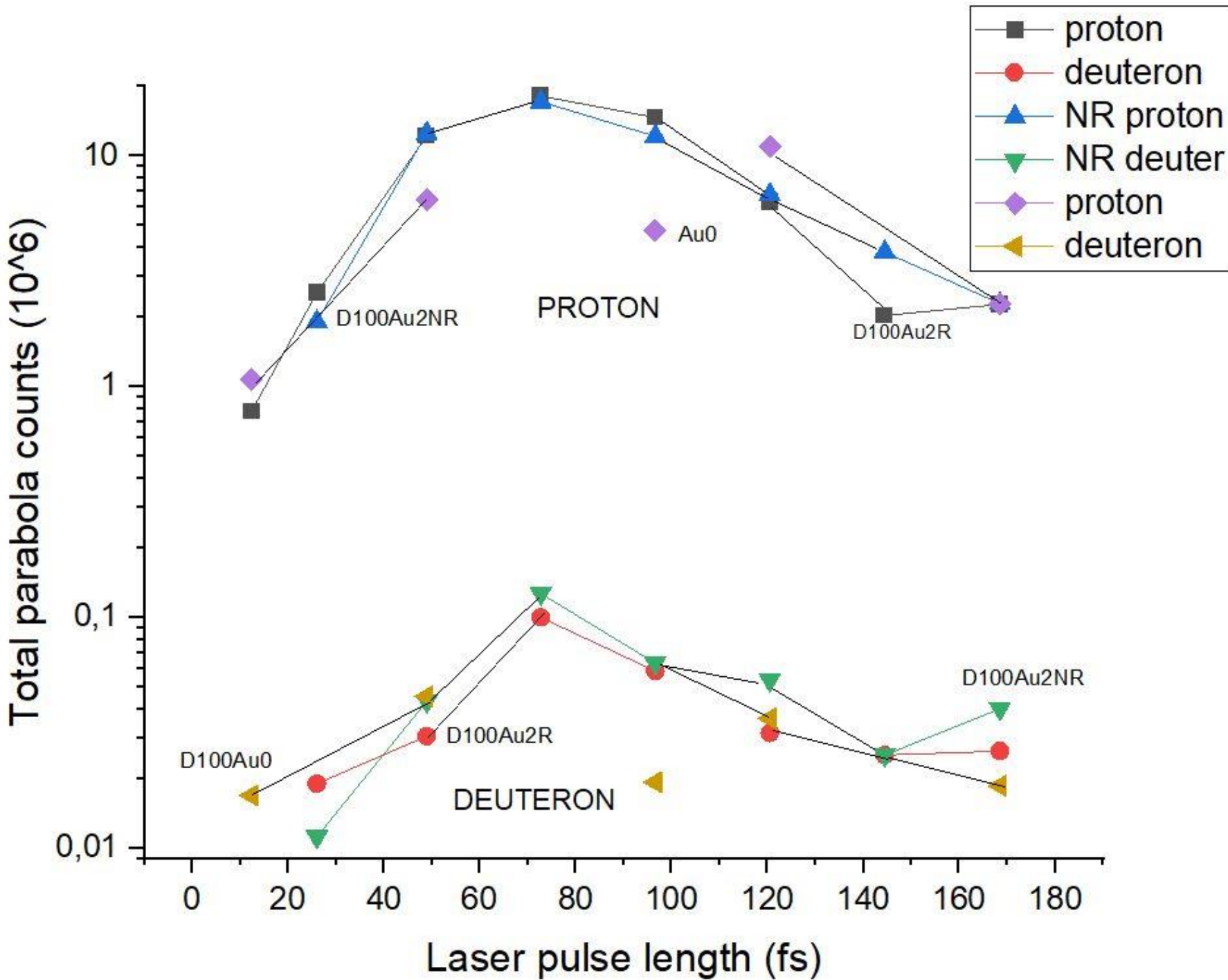
096

shot_2024-02-07-14-52-41-235599.tif

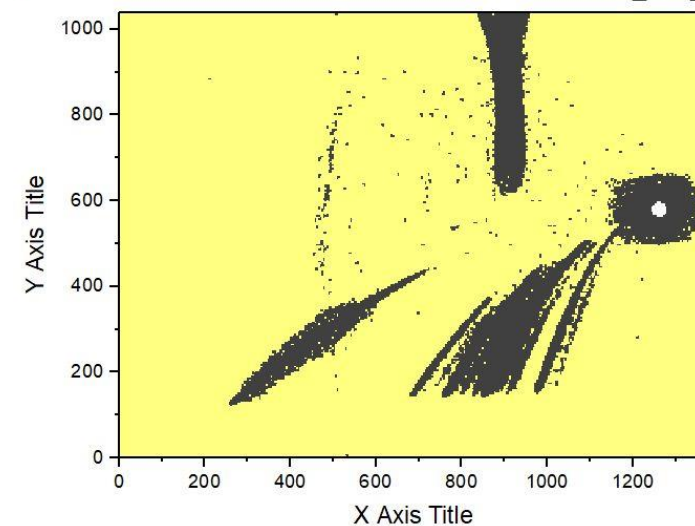
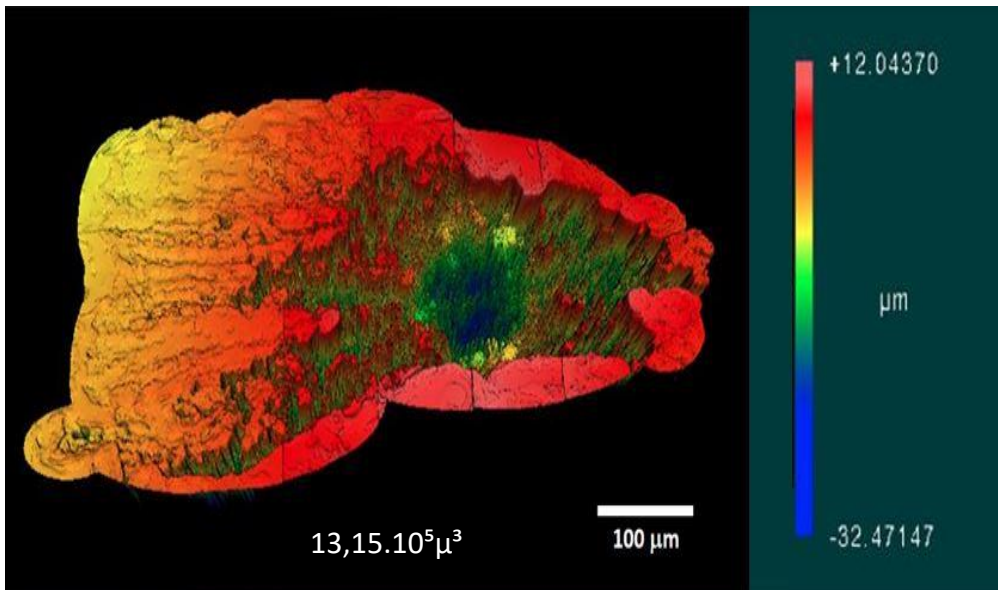


NO DEUTERIUM LINE SEEN!!!





096_shot_2024-02-07-

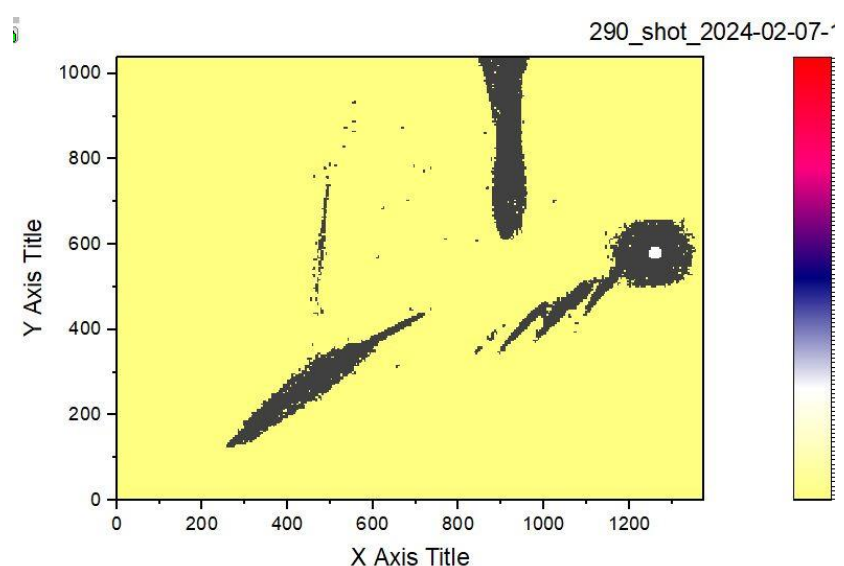
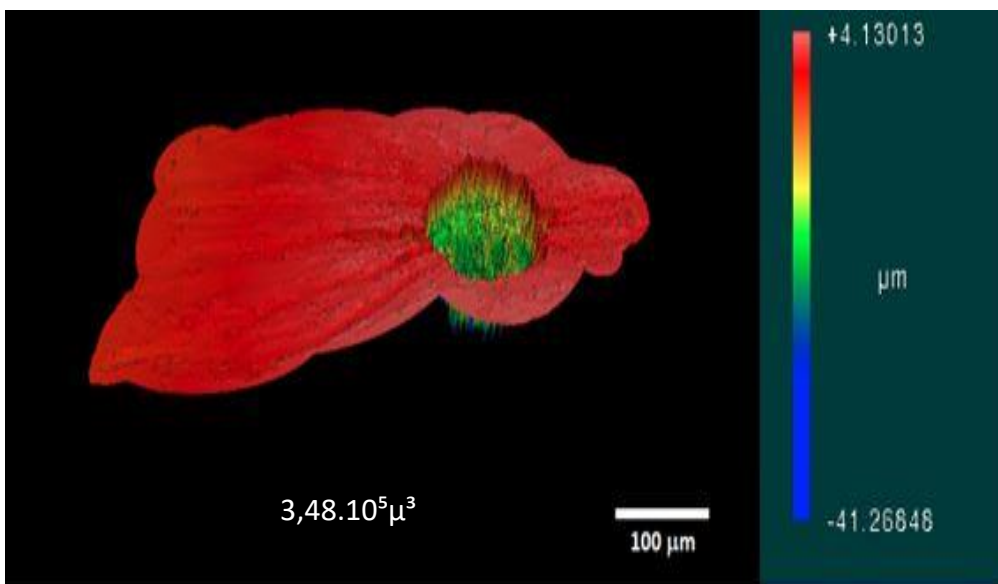


$$V_2/V_0 = 3.78$$

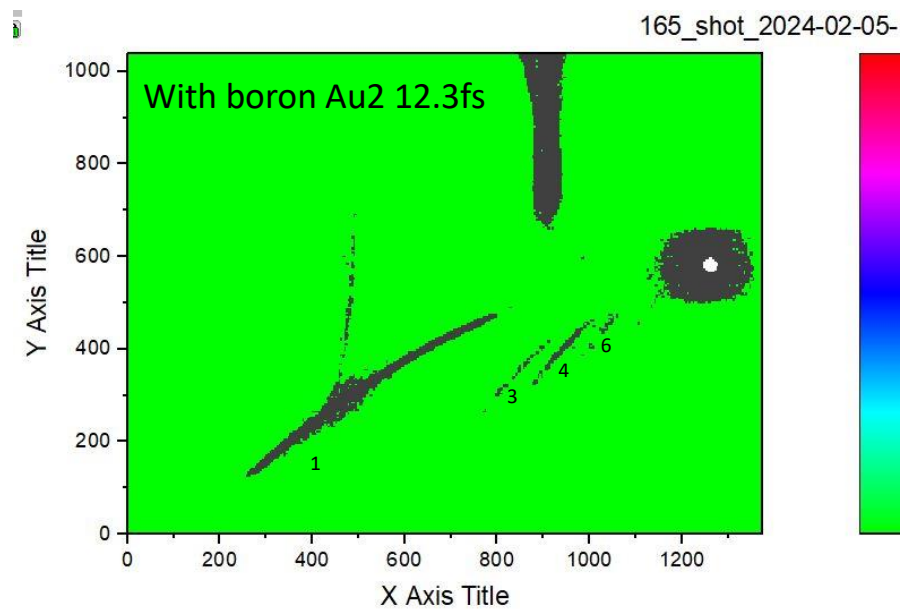
Laser pulse
length: 43fs

$$C_2/C_0 = 6.54$$

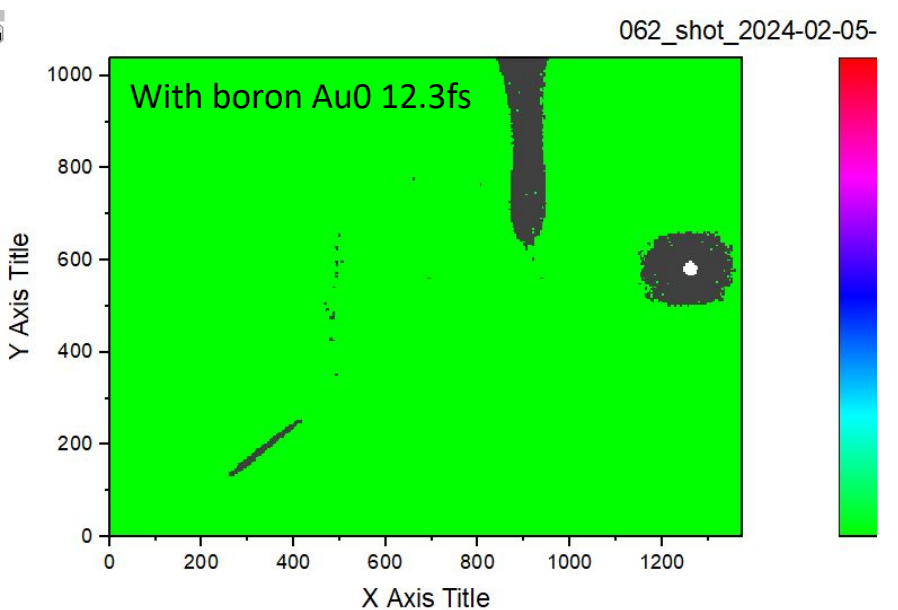
Total: =~ 2



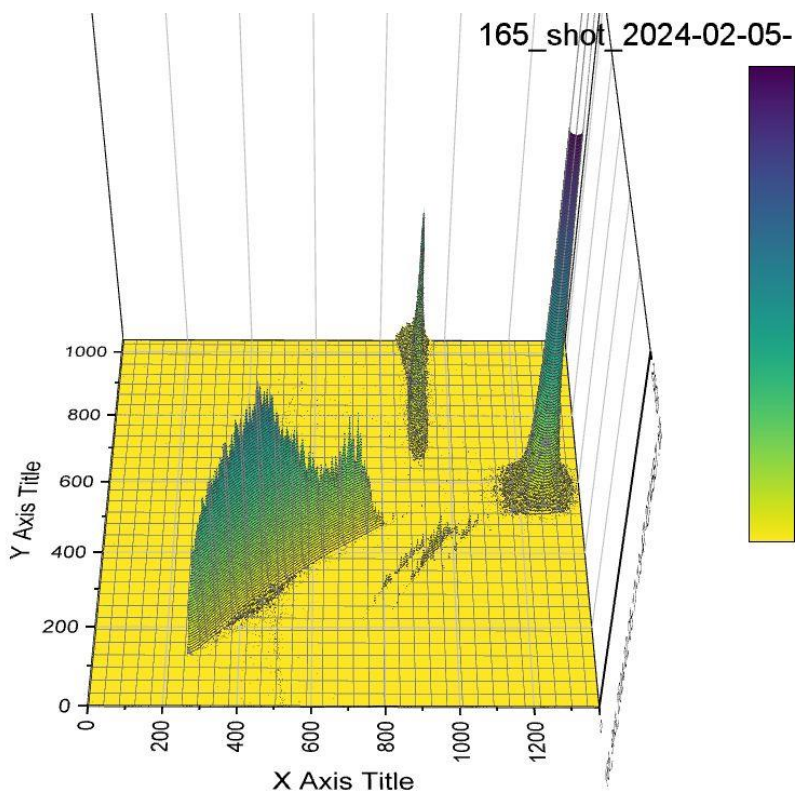
165_shot_2024-02-05



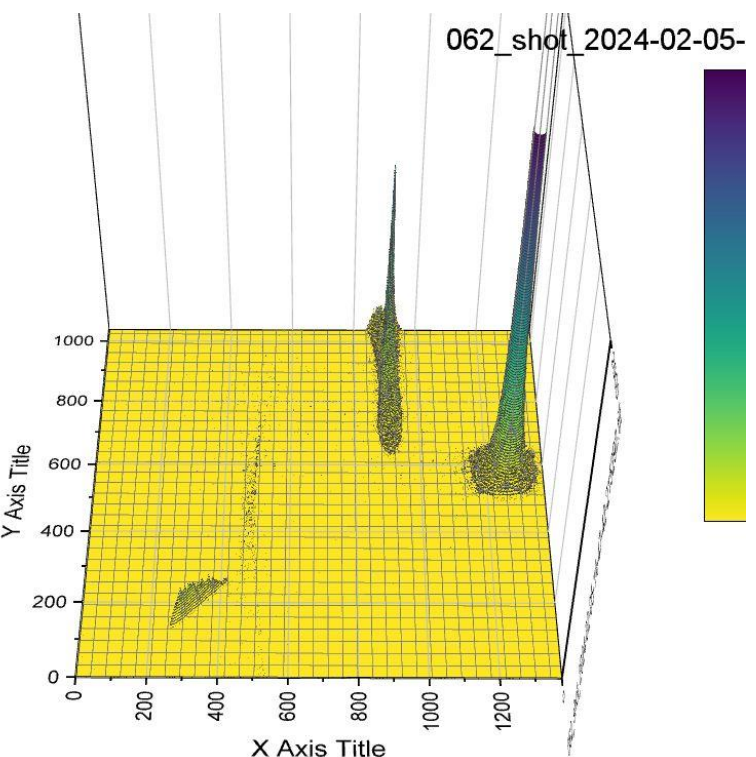
062_shot_2024-02-05

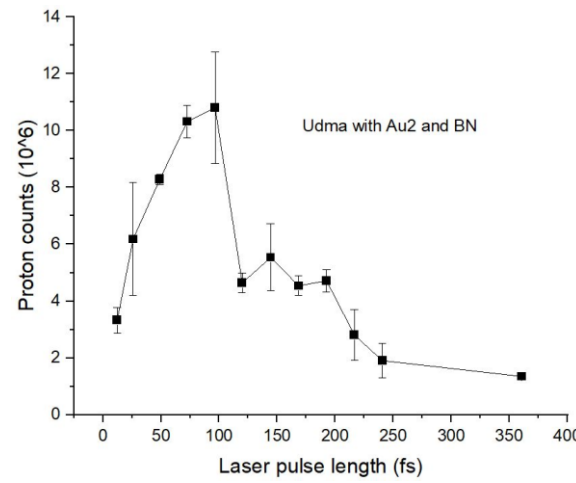
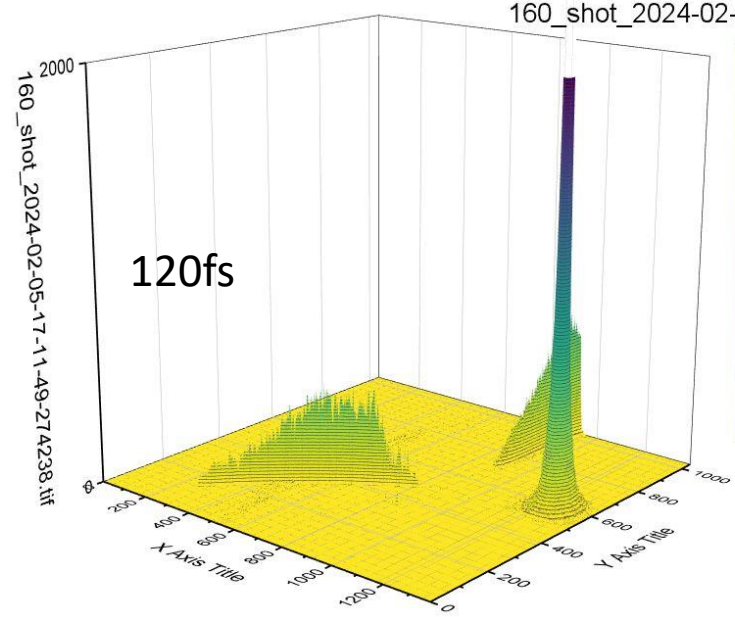
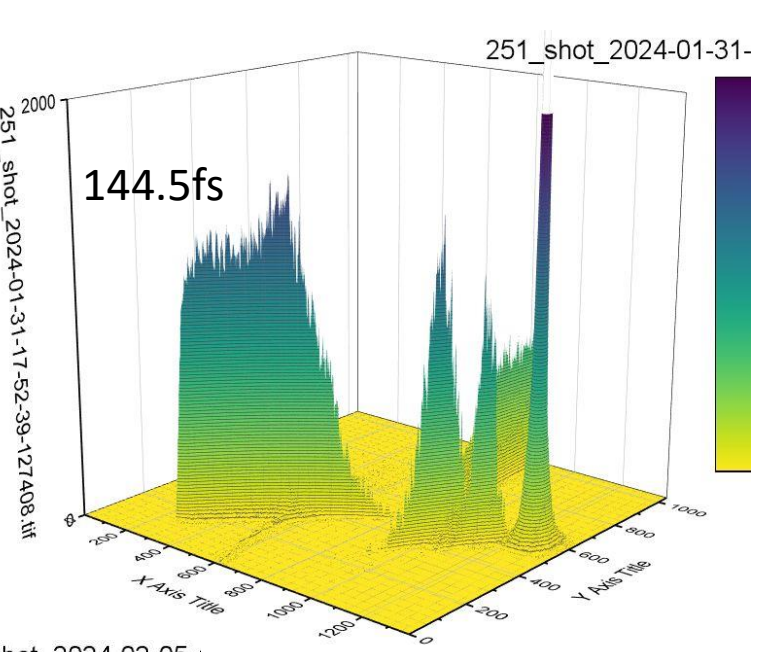
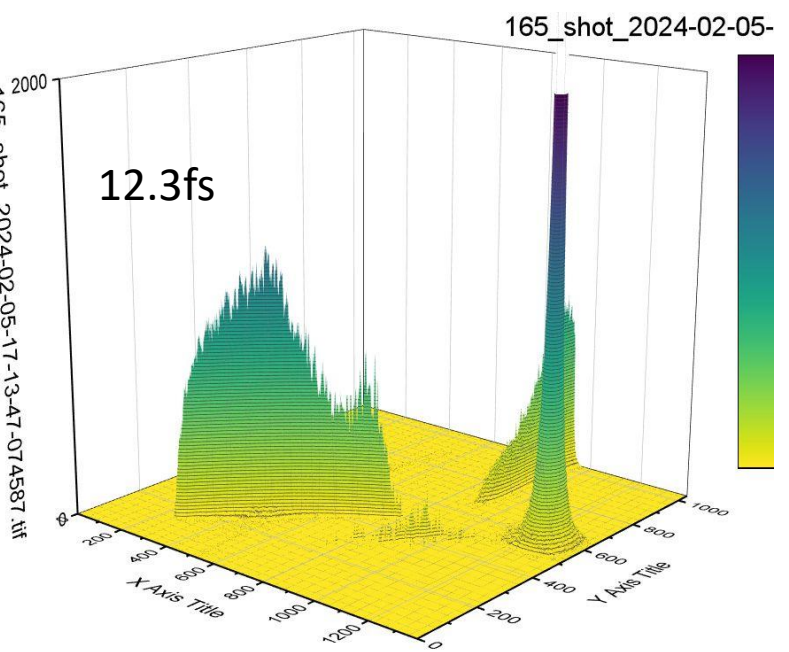


165_shot_2024-02-05

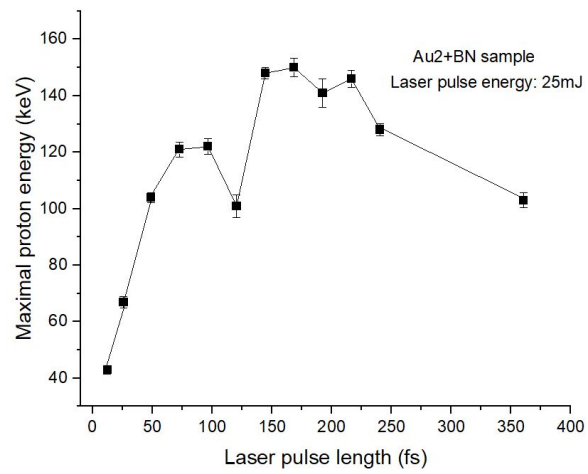


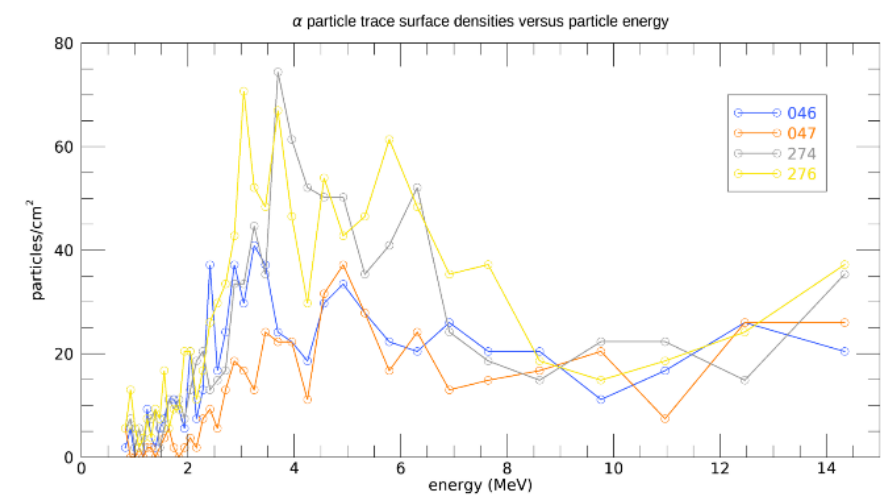
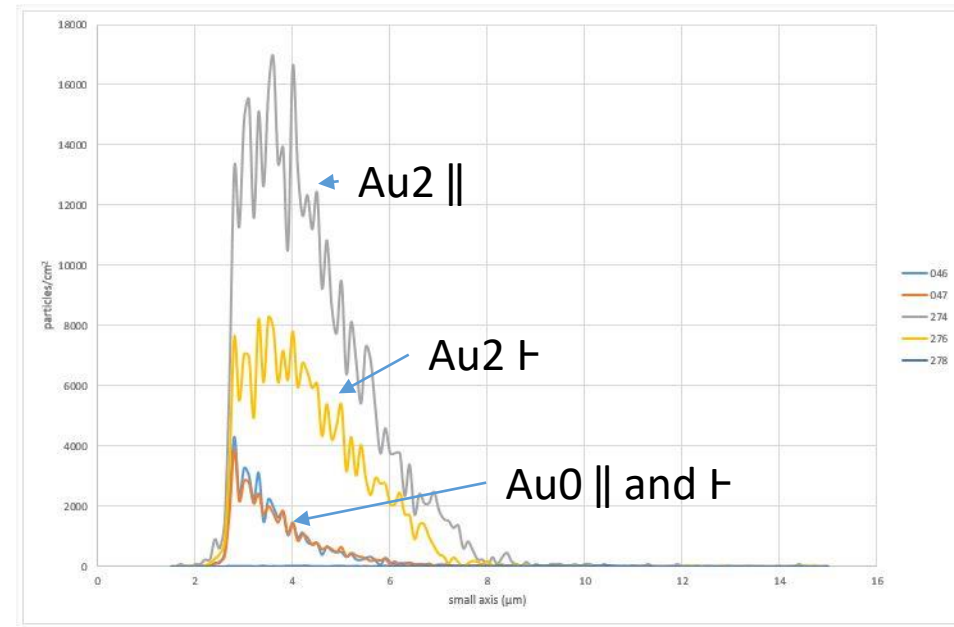
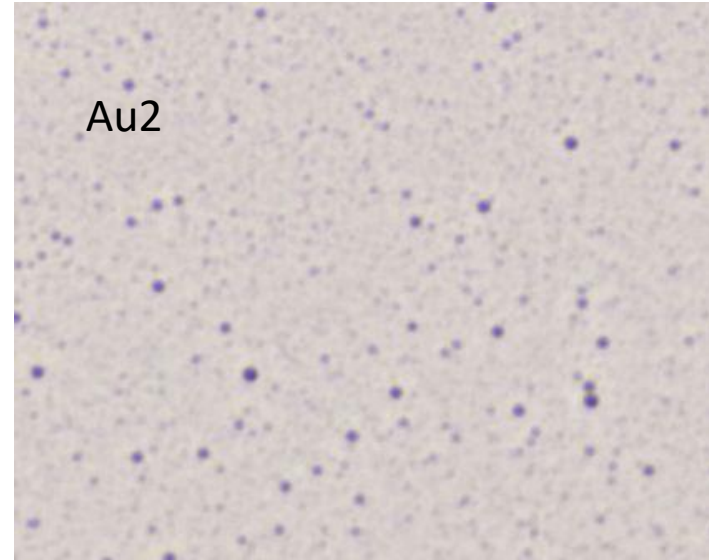
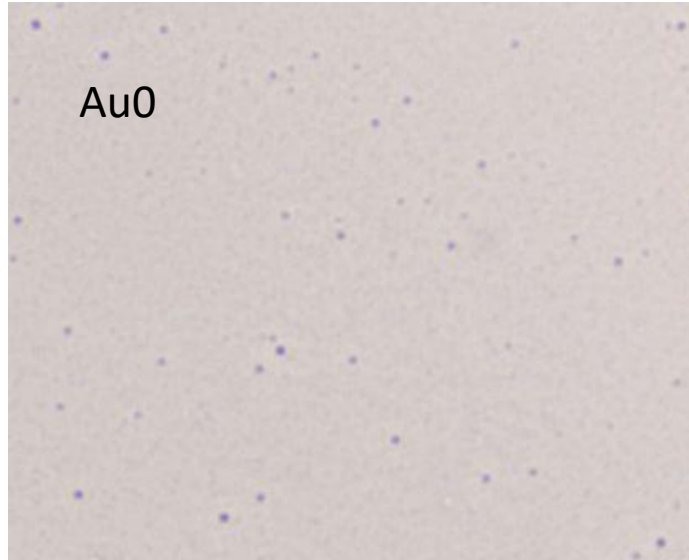
062_shot_2024-02-05



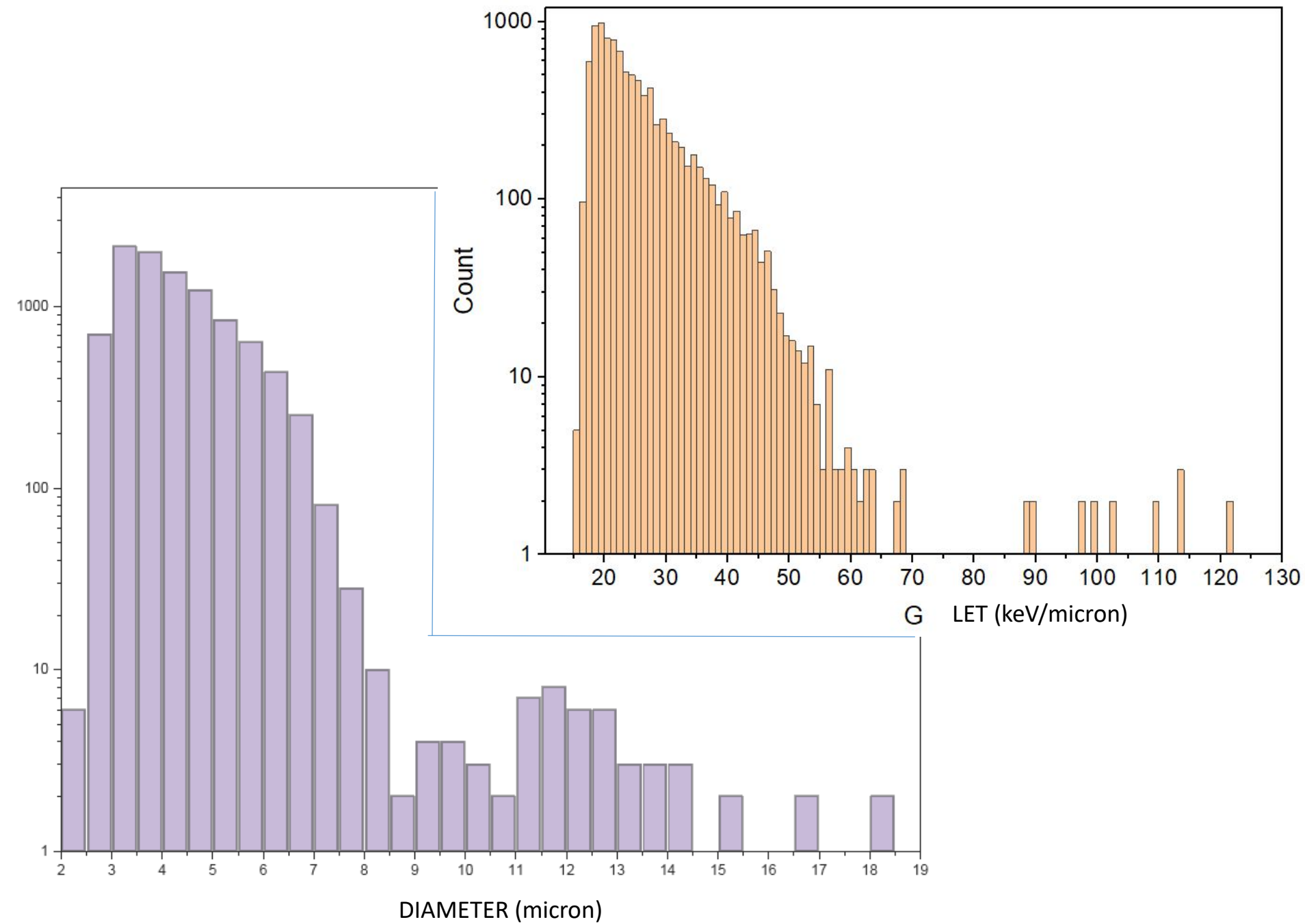


Samples with Au2 and BN





G



CONCLUSIONS

1. Table-top lasers have been found to indicate the significant role of high field nanoplasmonics in potential nuclear fusion processes.
2. Above $\sim 10^{17} \text{W/cm}^2$ laser intensity the formation of the reflective plasma mirror is negligible, light penetrates into the sample.
3. Plasmonics works also at high laser intensities.
 - Significant energy production has been detected, indicated by the increase of the crater volume and higher particle energies in the Thompson parabola results (also in BN seeded samples).
 - The source of this excess energy could be partly the deuterium production, detected by 2 optical spectroscopy methods.
 - The particle energy of ions in the plume is always higher for samples with resonant plasmonic nanoparticles than for those without them.
 - The Thomson parabola spectrometer data indicate also this influence of the LSPP resonance effect on the basic processes.
4. Some preliminary results on nuclear processes have also been shown, but here further, more detailed studies are needed.
5. Several other studies are planned (nanoparticle size and material , direct nuclear detection of alfa particles, etc.)

THANKS FOR YOUR ATTENTION!



When the winds of changes are blowing some build shelters,
but some others build wind turbines

